

# Utilizing Chemical Optical Sensor Technology to Assess Oxygen Permeability of Candidate Asteroid Regolith Sample Containers

Christopher J. Snead<sup>1</sup>, Kevin Righter<sup>1</sup> and Nicole Lunning<sup>1</sup>

<sup>1</sup>*NASA Johnson Space Center*

The Astromaterials Acquisition and Curation Office at NASA Johnson Space Center currently curates 500 mg (10%) of carbonaceous asteroid Ryugu regolith collected by the Japan Aerospace and Exploration Agency's Hayabusa II spacecraft and returned to Earth in 2021 [1]. In September 2023, NASA's OSIRIS-REx spacecraft is expected to return at least 60 grams of regolith collected from the surface of Carbonaceous Asteroid Bennu [2]. These new astromaterials collections will be stored and handled in gloveboxes and desiccators that are continuously purged with ultrapure nitrogen, in order to minimize contamination and alteration of extraterrestrial samples from terrestrial environments, e.g. reaction with terrestrial oxygen. Ito et al. have previously reported on the development of containers to transport samples between facilities in inert, sealed environments [3]; Hayabusa2 samples allocated to investigators by JAXA's Extraterrestrial Sample Curation Center (ESCuC) are shipped in these Facility-to-Facility Transfer Containers (FFTCs). NASA curation has also been investigating sealed containers for storage, transportation, and allocation of Bennu and Ryugu regolith in sealed anoxic environments. In order to assess the ability of potential sample containers to maintain an inert atmosphere, we have acquired a PreSens Fibox 4 fiber optic oxygen meter and PSt9 chemical optical sensor spots. Oxygen measurements are performed as follows: A calibrated PSt9 sensor spot is fixed either mechanically or with adhesive to an internal transparent container surface (the container must incorporate at least one transparent surface into its design, i.e. the container cannot be completely opaque). The end of the oxygen meter's fiber optic attachment is placed normal to the exterior transparent face (opposite the sensor spot), and a measurement is made. This configuration provides a passive, non-invasive method of measuring an unmodified sample container [4]. The sensor can perform multiple measurements in time intervals as short as one second; by measuring the oxygen concentration of the internal container volume periodically, we can determine a rate of oxygen ingress into candidate sample containers. The PSt9 sensor has a measurement range of 0-200 ppmv; we therefore seal our containers and measure the internal sensor within a nitrogen purged glovebox. We compare the reading for the sealed container with a control sensor spot that is loose in the glovebox. The sealed container is then removed from the glovebox (as well as the fiber optic O<sub>2</sub> meter), and measurements are made in periodic intervals of 10 minutes to one hour (depending on ingress rate) to assess changes in the internal oxygen environment. We conducted very preliminary tests on a commercial stainless steel container sealed with a Viton gasket; an internal oxygen concentration of 200 ppmv was measured four days after removal from the ~30ppm glovebox environment. More controlled experiments are required to determine whether the increase in oxygen was due to diffusion through the Viton gasket, or whether outgassing internal contaminants contributed to the increased oxygen concentration; these experiments will be conducted in October 2022.

## References

[1] Watanabe S. et al. 2017. Space Sciences Reviews, 208, p. 3-16. [2] Lauretta D. S. et al. 2017. Space Sciences Reviews, 212, p. 925-984. [3] Ito M. et al. 2020. Earth, Planets and Space. 72:133. [4] Huber C. et al. 2006. Monatschrift für Brauwissenschaft, 59, 5-15.

# Space Resources – From the Moon to Near-Earth Asteroids and Back

Dennis Harries<sup>1</sup>

<sup>1</sup>European Space Resource Innovation Centre (ESRIC), Luxembourg Institute of Science and Technology/Luxembourg Space Agency. 41, rue du Brill, 4422 Belvaux, Luxembourg (dennis.harries@esric.lu)

Space exploration is a frontier that challenges creative and sustainable use of extraterrestrial materials. Whilst space missions during the past decades entirely relied upon supplies brought from Earth, future missions aiming at long-term human and robotic activity outside of Earth's atmosphere require technologies to produce propellants, life support, and construction materials from local extraterrestrial resources. This in-situ space resource utilization (ISRU) is key for the exploration of the Moon and Mars and to make space transportation more economical and environmentally sustainable. Examples are in-orbit fuelling and refuelling of spacecrafts, as well as the resource-efficient and circular processing of materials for building habitats and photovoltaic energy infrastructures.

The Moon's south polar region will a primary target for long term exploration starting with the international Artemis missions led by NASA. This area is particularly interesting due to its permanently shadowed regions (PSRs) inside polar craters, which are expected to hold water ice and other volatiles trapped by the very cold temperatures within. Remote sensing and the impact experiment of NASA's LCROSS mission places constraints on the amount and composition of volatiles, confirming the presence of water ice at several volume percent of the regolith [1]. Hydrogen gas produced from PSR ices or imported from Earth is the basis of oxygen generation from lunar ilmenite through redox reaction ( $\text{FeTiO}_3 + \text{H}_2 \rightarrow \text{Fe} + \text{TiO}_2 + \text{H}_2\text{O}$ ) and electrolysis of the produced water. Alternative to this is the electrolysis of lunar regolith itself in the FFC Cambridge process employing a molten calcium chloride electrolyte. The FFC process reduced not only ferrous oxides but almost the entire oxide components of the regolith to produce a high yield of oxygen. Both processes require volatiles (hydrogen, chlorine) that need to be efficiently recycled due to their limited abundance on the lunar surface.

Carbon and nitrogen compounds such as  $\text{CO}_2$  and  $\text{NH}_3$  are present in PSRs, but their overall abundance is uncertain and in case of  $\text{CO}_2$  suitable traps may be rare [2]. With typical carbon and nitrogen concentration of 10s to a few 100s of ppm in the average lunar regolith, mainly through solar wind implantation, both elements are geochemically highly limited but, besides hydrogen, essential for life support and most propellants. For propellants a sustainable circularisation of volatiles is obviously not possible.

Ryugu and its potential near-Earth asteroid (NEA) siblings are now confirmed to contain up to ~6.8 wt%  $\text{H}_2\text{O}$  [3] chemically bound in serpentines and smectites. Up to ~4.6 wt% of carbon are present as carbonates and organic matter that also contains considerable amounts of nitrogen. As discussed above, hydrogen, carbon, and nitrogen are critical resources for extended lunar presence and chemical manufacturing of propellants in space. As carbon and nitrogen are especially limited on the lunar surface, the retrieval of such resources from NEAs might become a long-term option for a sustained space economy. These asteroids are comparably easy to reach with low  $\Delta v$  requirements from and into cis-lunar space [4]. Exploratory heating experiments of C-type chondritic meteorites using high-vacuum extraction and mass-spectrometric detection of released volatiles indicated complex release patterns of  $\text{H}_2\text{O}$ ,  $\text{CO}_2$ , CO and nitrogen compounds (Fig. 1). Thermodynamically valuable CO appears to be a major species and likely the result of redox reactions involving the carbonates, organic matter and magnetite. Extraction yields, energy requirements, and catalytic chemical conversion of this potential feedstock into further products, such as fuels and oxidizers, are some of the to-be-studied process constraints for NEA-based ISRU. Operating on small, nearly cohesionless rubble-pile asteroids is another extreme challenge for both small body exploration and any future ISRU.

## References

- [1] Colaprete A. et al. 2010. Science 330:463–468. [2] Schorghofer N. et al. 2021. Geophysical Research Letters 48:e2021GL095533. [3] Yokoyama T. et al. 2022. Science eabn7850. [4] Jedicke R. et al. 2018. Planetary and Space Science 159:28–42.

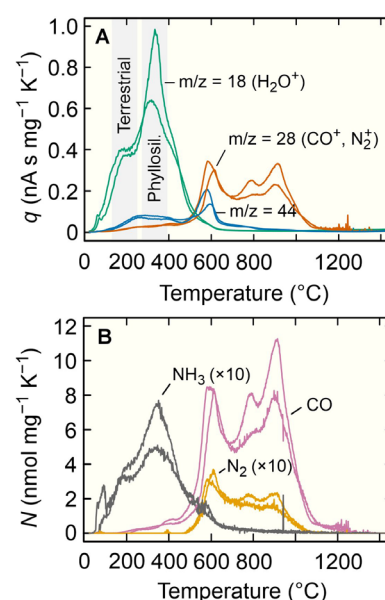


Figure 1: Volatile species detected by quadrupole mass spectrometry during controlled high-vacuum heating of the Murchison CM2 chondrite at 10 K/min. A. normalized ion currents. B. Species after fragment pattern deconvolution.

## Formation processes of spherulitic magnetite in the Ryugu samples

E. Dobricá<sup>1</sup>, H. A. Ishii<sup>1</sup>, J. P. Bradley<sup>1</sup>, K. Ohtaki<sup>1</sup>, T. Noguchi<sup>2,3</sup>, T. Matsumoto<sup>4</sup>, A. J. Brearley<sup>5</sup>, the Min-Pet Fine Sub-team and the Hayabusa2 initial analysis core

<sup>1</sup>*Hawai'i Institute of Geophysics & Planetology, University of Hawai'i at Mānoa, Honolulu, HI 96822, USA (dobrica@hawaii.edu)*, <sup>2</sup>*Division of Earth & Planetary Science, Kyoto University, Kyoto, Japan*, <sup>3</sup>*Department of Geology and Mineralogy, Kyushu University, Kyoto, Japan*, <sup>4</sup>*Hakubi Center for Advanced Research, Kyoto University, Kyoto, Japan*, <sup>5</sup>*Department of Earth and Planetary Sciences, University of New Mexico, Albuquerque, NM.*

**Introduction:** Samples returned from the carbonaceous asteroid 162173 Ryugu by the JAXA Hayabusa2 mission allow us to investigate primitive materials of our Solar System and their evolution [1-2]. Recent studies have shown that the Ryugu samples are composed of minerals similar to those of CI (Ivuna-like) carbonaceous chondrites indicating that the parent planetesimal from which Ryugu was derived experienced severe aqueous alteration [e.g., 1-2]. Our previous study described that magnetite in the Ryugu samples from chamber A occurs as framboids, plaquettes, spherulitic, and irregularly shaped grains [3-5]. They are products of alteration, and their formation is controlled by variation in the diffusion and growth rates during aqueous alteration on the parent body [4]. In this new study, we focus on spherulitic magnetite grains in the Ryugu from chamber C to understand the evolution of the aqueous alteration processes on the carbonaceous (C-type) asteroids [4].

**Samples and Methods:** Multiple spherulitic magnetite grains were identified embedded in the fine-grained materials returned by the Hayabusa2 spacecraft collected during both touchdowns (chambers A and C). Figure 1 shows the spherulitic magnetite (~13 µm in diameter) analyzed in this study and collected during the second landing operation (chamber C, C0105-039024). The grain is associated with fine-grained phyllosilicates, euhedral sulfides, and framboidal magnetites Fig. 1). We prepared one FIB section for electron microscopy studies using the Helios 660 dual-beam focused ion beam SEM (FIB-SEM) instrument at the University of Hawai'i at Mānoa and examined the section by transmission electron microscopy (TEM) using the JEOL NEOARM 200CF at the University of New Mexico.

**Results:** The spherulitic magnetite has an internal texture composed of individual radiating fibers varying in length from 5 µm to 8 µm. The fibers radiate from a spherical pore (Fig. 1, ~130 nm in diameter) located off-center. The widths of the fibers vary in size from 70 nm to 140 nm. The spherulitic magnetites are characterized by high porosity, with randomly distributed pores ranging from a few nanometers up to 2.2 µm in size; however, the magnetites with other morphologies (e.g., framboidal magnetite) are free of pores. Most pores are euhedral to subhedral in shape, located inside the fibers or at their boundaries. Additionally, we identified an amorphous rim (80- 350 nm in thickness) composed of 5 wt % Si, 4 wt% S, 2 wt% P, and 13 wt% C around the magnetite grain.

**Discussion:** Ryugu samples have been shown to a CI chondrite that exhibit some notable differences from CI meteorites [6-7]. One of the major similarities in Ryugu asteroid to CI chondrites is the presence of magnetites with different morphologies. Magnetite with a variety of morphologies has been studied for almost sixty years in one of the rarest groups of meteorites, the CI chondrites (only 9 meteorites belong to this group), and more recently in the unique, ungrouped Tagish Lake meteorite [8-9]. Our TEM observations further expand on the implications of magnetite formation in the Ryugu samples that show some difference to known CI chondrites [6-7]. The observations presented in this study show the presence of magnetite with different morphologies coexisting in close proximity.

Spherulites are common in terrestrial and extraterrestrial materials [8, 10-11]. They have been identified in a wide range of materials such as metals, alloys, polymers, oxides, liquid crystals, and various biological molecules. However, so far there is no generally accepted theory of spherulite crystallization mechanisms. The most important prerequisite for spherulitic growth is high crystallization driving forces, typical from a supersaturated or supercooled solution [11]. Furthermore, spherulites are ubiquitous in solids formed under highly nonequilibrium conditions [10, 12]. Systems that are in equilibrium tend to grow crystals with simple morphologies unless they are forced out of equilibrium by imposing a change in the environmental conditions [12]. Therefore, crystals can form complex spatial patterns in response to a disturbance from equilibrium that might induced kinetically driven growth to lower the free energy of the system. Though there are other factors that can influence the morphologies of crystals. For example, the presence of organic compounds can play a major role influencing growth of crystals by inhibiting growth on some crystal surfaces and favoring one morphology over another [6]. Similarly, it is also possible that certain anions or cations in solution can change the growth mechanism and change the morphology (Wark et al. 2008).

Previous studies of spherulites in meteorites suggested that this particular structure requires crystallization from a colloidal Fe hydroxide gel-like material [8]. Studies of terrestrial spherulite show that a viscous medium (i.e., gel) is not

always necessary for spherulitic growth; however, impurities encourage spherulite formation [11]. The conditions necessary for the spherulite precipitation must maintain the growth rates ( $G$ ) of the crystal itself higher than diffusion rates ( $D$ ,  $G \gg D$ ) [8, 13]. Any changes related to variation in  $D/G$  ratio could generate crystals with different morphologies [13]. Therefore, the presence of magnetite with varying crystal morphologies in the returned samples suggests a variable range of crystal growth and diffusion rates in the Ryugu parent body. Petrographic observations suggested that magnetites with a spherulitic morphology are the one of the first minerals to crystallize from an aqueous fluid on the Ryugu parent body [14]. More precisely, the crystallization sequence of magnetite as a function of their morphologies is: spherulitic – plaquette/framboidal – equant/elongated [14]. This previous study indicated that the conditions during magnetite precipitation changed from high to low supersaturations [14], which supports our observations that the first magnetites that formed, the spherulitic crystals, precipitated from a highly supersaturated fluid that evolved in the degree of saturation. Our TEM study further expands on these results suggesting that at the beginning of the crystallization sequence, when the spherulitic magnetite formed, the fluid could have been under nonequilibrium conditions. These processes lead to polycrystalline growth structures imposed by the reach of the solution of a supersaturated state where nucleation is able to occur, resulting in the adjustment to a lower free energy condition. Furthermore, as the previous petrographic observations suggested [14], and the presence of numerous fragile, euhedral laths at the surfaces of these spherulitic magnetites, suggest that these crystals precipitated first in an unrestricted, high porous material.

Two important implications arise from the study of spherulitic magnetite. First, these crystals could potentially offer a unique opportunity to study the early aqueous fluids that circulated through the Ryugu parent body. No materials were identified in the unique pores identified in the spherulitic magnetite due to the sample preparation technique applied in this study; however, it is possible that these pores contain fluid inclusions prior to the FIB sample preparation. A second important implication that arises from the occurrence of spherulitic magnetite under nonequilibrium conditions is that a careful selection of the magnetite crystals is necessary for the use of the oxygen isotope fractionation between carbonates and magnetite to extract the temperature at which these minerals coprecipitated [15]. Since multiple generations of magnetite were identified in the Ryugu samples, the question is what type of magnetite forms in equilibrium with the carbonates, especially since dolomite and breunnerite formed after the formation of pentlandite, pyrrhotite, and apatite according to the crystallization sequence [14]. We suggest avoiding spherulitic magnetite for these measurement since the necessary assumption of equilibrium between minerals is not supported by our observations indicating rapid magnetite growth.

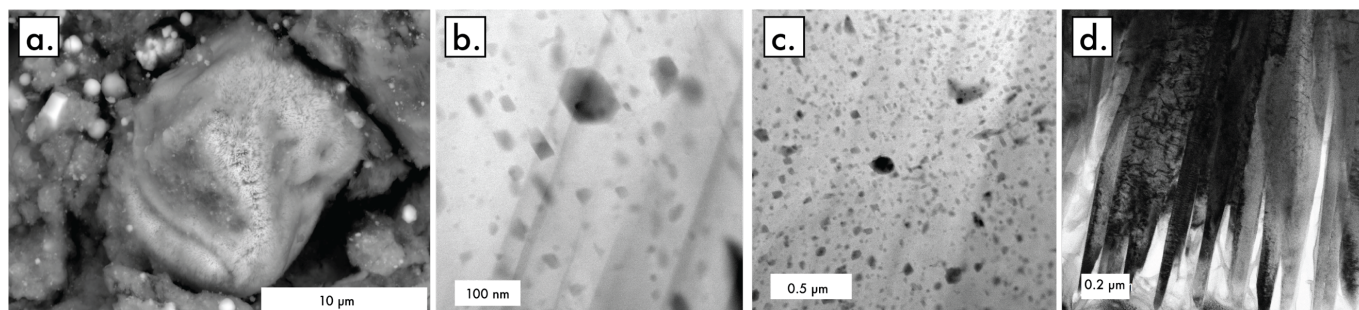


Figure 1. Backscattered electron (a), dark-field STEM (HAADF, b-c), and bright-field TEM images of the spherulitic magnetite analyzed in this study. The TEM data show the texture of the radiating fibers and the random distribution of euhedral to subhedral pores.

## References

- [1] Noguchi T. et al. (2022) 53rd LPSC, Abstract #1747. [2] Tachibana S. (2021) Sample Return Missions the Last Frontier of Solar System Exploration, Chapter 7, Elsevier, Editor Longobardo A., 147-162. [3] Alving J. et al. (2019) *Geochemistry*, 79, 125532. [4] Dobrica E. et al. (2022) 53rd LPSC, Abstract #2188. [5] Lee M. R. et al. (2022) 53rd LPSC, Abstract #2203. [6] Nakamura T. et al. (2022), *Science*, doi 10.1126/science.abn8671. [7] Yokoyama T. et al. (2022) *Science* 10.1126/science.abn7850. [8] Kerridge J. F. (1979) *Science* 205, 395-397. [9] Kimura Y. et al. (2013) *Nat. Comm.* 4, 1-8. [10] Gránásy L. et al. (2005) *Phys. Rev. E* 72, 011605. [11] Shtukenberg A. G. et al. (2012) *Chem. Rev.*, 112, 1805-1838. [12] Magill J. H. (2001) *J. of Mater. Sci.* 36, 3143-3164. [13] Lofgren G. (1974) *Americ. J. Sci.* 274, 243-273. [14] Tsuchiyama A. et al. (2022) 85th Annual Meeting of the Meteoritical Society, abstr. #6221. [15] Jilly-Rehak C. E. et al. (2018) *Geochim. Cosmochim. Acta* 222, 230-252.

# The Aguas Zarcas breccia - similarities to surface features of C-type asteroids Ryugu and Bennu

Imene Kerraouch<sup>1,2</sup>, Michael E. Zolensky<sup>2</sup> Addi Bischoff<sup>1</sup>

<sup>1</sup>*Institut für Planetologie, University of Münster, Wilhelm-Klemm Str. 10, D-48149 Münster, Germany.*

<sup>2</sup>*Astromaterials Research and Exploration Science, NASA Johnson Space Center, Houston TX 77058, USA  
(ikerraou@uni-muenster.de)*

Knowledge of the materials originally present in the protosolar nebula is one of the most significant constraints for models of the formation of our solar system. The physicochemical properties of these original materials can be determined through two different and complementary approaches: (a) astronomical observations of nascent stellar systems and the dense clouds from which they originated and (b) laboratory studies of available astromaterials such as meteorites, interplanetary dust particles, comet coma grains, including returned mission samples (e.g., from Hayabusa -1 -2; OSIRIS-Rex). Laboratory study of these extraterrestrial materials provides valuable information about the first solid materials of the early solar system and their evolution. Here, we present petrographic and mineralogical characteristics of work on the polymict carbonaceous breccia Aguas Zarcas [1].

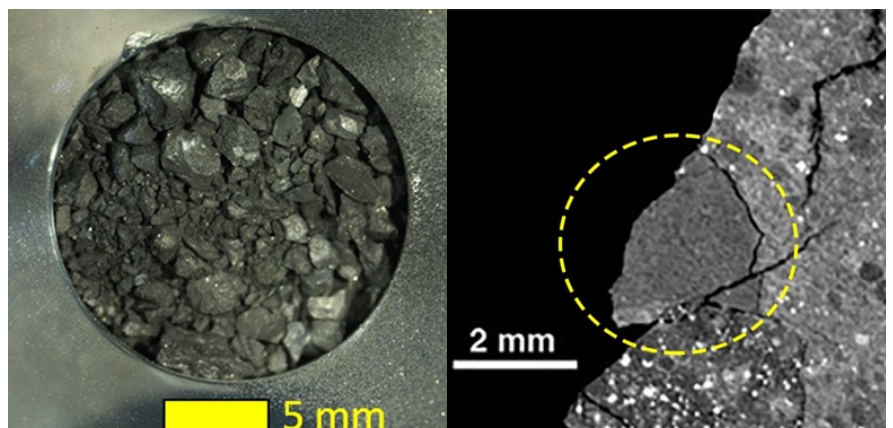
On April 23, 2019, at 21:07 local time, a meteorite fall occurred in Aguas Zarcas, San Carlos County, Alajuela province, Costa Rica. The rapid recovery of this brecciated carbonaceous chondrite after its fall provides an opportunity to investigate a freshly fallen, relatively uncontaminated, and highly-brecciated meteorite to compare with samples returned by the Hayabusa2 and OSIRIS-REx spacecraft from C-complex asteroids.

This study includes the examination of several pre-rain fragments. X-ray computed tomography (XCT) results show numerous different lithologies [1]. In this study, we describe the petrography and mineralogy of five different lithologies of the Aguas Zarcas meteorite. We also present data on the bulk oxygen isotopes of some of these lithologies. We describe all fragments in detail and attempt a classification of each lithology in order to better understand the origin and formation history of the Aguas Zarcas parent body.

Our results show that some lithologies of Aguas Zarcas are similar to those in CM chondrites, but others are unique. The different lithologies [1] also represent different degrees of hydration and heating, which are good analogues for the types of material returned from asteroids Bennu and Ryugu.

Spectroscopic observations of Ryugu and Bennu compared to laboratory measurements of meteorites suggest that the asteroids have some similarities to heated CM, heated CI, or CI chondrites [2-5]. Both asteroids are thought to be composed of materials altered by aqueous alteration (e.g., [5]) and formed by reaccumulation after destruction by impacts and brecciation (e.g., [6-7]). Considering the different lithologies in Aguas Zarcas [2] and other CM chondrites [8-9], these types of carbonaceous chondrites can be considered good analogues for samples from Ryugu and Bennu. The presence of unique and rare lithologies in Aguas Zarcas, different from typical CM chondrite lithologies, requires complex mixing of different materials in a highly dynamic environment.

Fig.1: Left image: sample catcher chamber A from Hayabusa2, captured by an optical microscope, shows many particles larger than 1 mm (Photo by JAXA Dec. 24, 2021). The right image: XCT image of a sample of Aguas Zarcas, showing a dark homogeneous C1-clast (marked by a circle) (Kerraouch et al., 2021; 2022). Both materials exhibit a mixture of different lithologies resulting from impact fragmentation, mixing, and reaccumulation during the evolution of their parent bodies.



**References** [1] Kerraouch et al., 2021. *Meteoritics & Planet. Sci.* 56, 277-310; [2] Kitazato et al., 2019. *Science* 364, 272–275; [3] Matsuoka et al., 2015. *Icarus* 254. 135–143; [4] Hanna et al., 2019. LPI abstract #2029; [5] Hamilton et al., 2019. *Nature Astronomy*. 3.332–340; [6] McCoy et al., 2019. *Metsoc54 abstract #6428*; [7] Michel et al., 2020. *Nature* 11, 2655; [8] Kerraouch et al., 2019. *Chemie der Erde* 79, 125518; [9] Lentfort et al., 2020. *Meteoritics & Planetary Sci.* 56, 127-147.

## **An Astromaterial Curation Facility at MNHN-Paris, the National Center for Extraterrestrial Material**

J. Duprat<sup>1</sup>, M. Roskosz<sup>1</sup>, B. Doisneau<sup>1</sup>, S. Pont<sup>1</sup>, M. Verdier-Paoletti<sup>1</sup>, S. Bernard<sup>1</sup>, M. Gounelle<sup>1</sup>, J. Aléon<sup>1</sup>, P. Sans-Jofre<sup>1</sup>, G. Avice<sup>2</sup>, F. Moynier<sup>2</sup>, R. Brunetto<sup>3</sup>, F. Poulet<sup>3</sup>, C. Engrand<sup>4</sup>, L. Delauche<sup>4</sup>, E. Dartois<sup>5</sup>

<sup>1</sup>*IMPMC, CNRS-MNHN-Sorbonne Université, UMR 7590, 57 rue Cuvier, 75005 Paris, France* ; <sup>2</sup>*Université Paris Cité, Institut de physique du globe de Paris (IPGP), CNRS, 75005 Paris, France* ; <sup>3</sup>*IAS, Université Paris-Saclay, CNRS, UMR 8617, Orsay, France* ; <sup>4</sup>*IJCLab, Université Paris-Saclay, CNRS/IN2P3, Orsay, France* ; <sup>5</sup>*ISMO, Université Paris-Saclay, CNRS, Orsay, France*

The study of extraterrestrial samples requires developments in curation facilities to preserve, and allocate pristine samples to international scientific teams. During the last decades, the return to Earth of samples from the Stardust NASA mission [1], Hayabusa1 and Hayabusa2 JAXA missions (e.g. [2, 3]), allowed the first analysis of samples from an identified comet (81P/Wild2) and from two asteroids (Itokawa and Ryugu). Within the coming years, samples from asteroid Bennu will return to Earth thanks to the OSIRIS-REx NASA-led mission [4] and, on a longer term, samples from the Martian moon Phobos will be returned by the MMX JAXA-led mission [5]. After 2030, material currently sampled at the Martian surface is expected to be returned to Earth by the NASA/ESA Mars Sample Return (MSR) campaign [6]. Major curation facilities already exist at both NASA and JAXA [7-9] to receive, curate and handle samples directly returned from space missions. Advanced curation studies are ongoing [9, 10] while others facilities are currently into construction [11]. Beside space missions, extraterrestrial materials (meteorites and cosmic dust) have been collected for centuries in many environments, including hot and cold deserts, deep sea sediments, sediments, polar ice caps, and stratospheric collections [12-14]. As recently illustrated by the striking similarity between Ryugu samples and the CI1 meteorites [15, 16], the comparison between returned samples (i.e. with known parent body) and meteorites or micrometeorites from terrestrial collections is an essential step in our understanding of these complex objects.

Together with the French spatial and scientific research agencies (CNES and CNRS), the Institut de physique du globe de Paris (IPGP) and Sorbonne University, the National Museum of Natural History (MNHN) launched a project to build a national curation facility, the CENAME (National Center for Extraterrestrial Materials) located at MNHN in the center of Paris. The CENAME will include instruments and advanced storage facilities developed by several French laboratories, including IAS and IJCLab at University Paris-Saclay. The CENAME will be designed to ensure long term curation of different major collections of extra-terrestrial samples including: the national meteorite collection from MNHN, large micrometeorites collections from Greenland and Antarctica, terrestrial analogues and samples from past and future space missions. The MNHN hosts an historical meteorite collection with more than 1500 different meteorites, including 521 falls, and a rich panel of Martian samples (Shergottites, Chassignites, Nakhilites) [17]. It contains the largest sample of the Orgueil CI-chondrite, a reference for cosmochemistry studies. The MNHN meteorite collection is actively used for cosmochemistry research projects and is constantly growing with new additions every year. Thanks to the pioneering work of M. Maurette in the 80s, large numbers of micrometeorites (interplanetary dust reaching Earth surface) with diameters ranging from a few tens up to a few hundred  $\mu\text{m}$  have been recovered from both Greenland and Antarctica [18, 19]. Since 2000, this program was pursued, in the central regions of Antarctica, where collections have been performed with the support of the French polar institute (IPEV) [20, 21]. The Concordia micrometeorites collection contains thousands of particles. A part of this collection is now fully characterized and contains micrometeorites with minimal terrestrial weathering, including particles of cometary origin that are exceptionally rich in organic matter (Ultra-Carbonaceous micrometeorites [22, 23]). The Concordia Collection is currently stored in a dedicated cleanroom at IJCLab in Orsay and will be transferred to the CENAME when the facility will be completed. The CENAME will also host a suite of terrestrial natural and synthetic analogues that are essential for analysis of complex extraterrestrial matter, calibration and interpretation of remote sensing analyses (e.g. on Mars). The CENAME will benefit from the MNHN Geological collection of rocks and minerals located in the same building. It contains about a billion scientific samples accumulated over 2 centuries of worldwide scientific exploration. The collection has been recently enriched with samples recording early Earth surface environments and the earliest traces of life on Earth (more than 1200 specimens spanning 3.5 billion years of Earth History). Beside these natural

samples, several laboratories involved in the CENAME project have developed dedicated experimental protocols to synthesize analogues of asteroidal and cometary organic matter.

Beyond these historical and on-going collections, the objective of the CENAME will be to allow sample handling, pre-characterization and long-term preservation for the next generations of samples for current and future space missions. As a result of on-going agreements between JAXA and the French space agency CNES, a fraction of Phobos (MMX) samples are expected to be transferred to the CENAME at MNHN after the period of initial description at JAXA-ISAS sample receiving laboratory and after the first scientific analysis by the MMX Science Sub-Teams (i.e. after 2030). The design of the CENAME will be modular to allow flexible configuration of different environments for the curation of pristine samples from other space missions. The CENAME will consist in a clean-room infrastructure of about 180 m<sup>2</sup>, divided in separated modules with ISO7 to ISO5 [24] environments, together with a laboratory for sample preparations and experiments that do not require a cleanroom environment. The cleanroom area will contain secured cabinets and glove boxes under controlled atmospheres (dry and purified N<sub>2</sub>, Ar, vacuum, ...). In the long-term perspective of MSR, an ambitious program was recently launched, under the supervision of CNES, to study an apparatus for small sample (solid and gas) handling in clean and bio-contained (BSL4-like) environment. The CENAME will include a dedicated space to allow rehearsal on such type of apparatus (before their operation in BSL4-like laboratories).

Instrumentation in the CENAME will focus on acquisition of the basic properties on samples with sizes going from  $\mu\text{m}$  to cm scales. It will include optical 2D and 3D microscopy and imaging, weighting, magnetic susceptibilities, scanning electron microscopy, Raman and infrared (IR) microspectroscopy with a dedicated suite of instruments, to achieve initial characterization and cataloging of samples before allocations. The magnetic environment of the samples and the magnetic properties of the handling tools will be monitored to ensure preservation of the genuine magnetic properties of the samples. A strict control of terrestrial contamination within CENAME cleanrooms will be achieved by real-time monitoring of inorganic, organic and biological contamination. The CENAME will develop research programs to improve existing curation techniques and new technological solutions for the mid to long-term curation of volatile elements (e.g., H<sub>2</sub>O, N, noble gases) contained in samples collected by future space missions (e.g. ice and gas from cometary objects or planetary atmospheres). Specific tasks will include the characterization of materials outgassing properties. A specific setup will be developed at IAS in order to allow a multi-scale (from mm down to  $\mu\text{m}$ ) IR reflectance micro-imaging characterization on the CENAME samples. The analysis will be fully non-destructive and non-invasive, and it will be performed within a dedicated bench in a controlled atmosphere (e.g., N<sub>2</sub>), with no need for specific sample preparation. In the case of returned samples, the setup will allow measurements complementary to the IR characterization performed at other curation facilities hosting the main sample collection (e.g., JAXA [25]).

**Acknowledgement:** The CENAME is a joint project supported by MNHN, IPEG, Sorbonne University, University Paris Cité, CNES and CNRS. The curation-related instruments and apparatus currently under development benefit from funding by Région Ile de France (DIM-ACAV<sup>+</sup> contract C<sup>3</sup>E), CNES, CNRS, MNHN and ANR contract (COMETOR 18-CE31-0011). The collection of micrometeorites benefited from the pluri-annual funding by IPEV and PNRA (Program #1020)

**References :** [1] Brownlee D. (2014) *Ann. Rev. Earth Planet. Sci.* **42**, 179-205. [2] Yano H., *et al.* (2006) *Science* **312**, 1350-1353. [3] Watanabe S., *et al.* (2019) *Science*, eaav8032. [4] Lauretta D.S., *et al.* (2017) *Space Sci. Rev.* **212**, 925-984. [5] Kuramoto K., *et al.* (2022) *Earth, Planets and Space* **74**, 12. [6] Beatty D.W., *et al.* (2019) *Meteorit. Planet. Sci.* **54**, S3-S152. [7] Yada T. *et al.* *Meteorit. Planet. Sci.* **49**, 135-153 [8] Evans C., *et al.* (2018) **42**, B4.2-49-18. [9] McCubbin F.M., *et al.* (2019) *Space Sci. Rev.* **215**, 48. [10] Hutzler A. *et al.* *EURO-CARES D7.1 Final technical Report*. [11] Helbert J., *et al.* (2020), EPSC2020-250. [12] Bland P.A., *et al.* (1996) *Mon. Not. R. Astron. Soc.* **283**, 551-565. [13] Brownlee D.E. (2016) *Elements* **12**, 165-170. [14] Taylor S., *et al.* (2016) *Elements* **12**, 171-176. [15] Nakamura T., *et al.* (2022) *Science* 10.1126/science.abn8671. [16] Yokoyama T., *et al.* (2022) *Science*, 10.1126/science.abn7850. [17] Caillet Komorowski C.L.V. (2006) *Geol. Soc. London Spec. Pub.* **256**, 163-204. [18] Maurette M., *et al.* (1986) *Science* **233**, 869-872. [19] Maurette M., *et al.* (1991) *Nature* **351**, 44-47. [20] Duprat J., *et al.* (2007) *Adv. Space Res.* **39**, 605-611. [21] Rojas J., *et al.* (2021) *Earth Planet. Sci. Lett.* **560**, 116794. [22] Duprat J., *et al.* (2010) *Science* **328**, 742-745. [23] Dartois E., *et al.* (2018) *Astron. Astrophys.* **609**, A65. [24] ISO 14644-1 [25] Yada T., *et al.* (2022) *Nature Astronomy* **6**, 214-220.

## Distinct ages and temperatures of aqueous activities recorded in Ryugu samples

Kazuhide Nagashima<sup>1</sup>, Noriyuki Kawasaki<sup>2</sup>, Naoya Sakamoto<sup>2</sup>, Wataru Fujiya<sup>3</sup>, Hisayoshi Yurimoto<sup>2</sup>, The Hayabusa2-initial-analysis chemistry team, and The Hayabusa2-initial-analysis core.

<sup>1</sup>University of Hawai'i at Mānoa<sup>1</sup>, <sup>2</sup>Hokkaido University, <sup>3</sup>Ibaraki University

The Ryugu asteroid is a rubble pile body likely composed of materials ejected by impact(s) from a larger parent asteroid [e.g., 1] that may have formed far from the Sun [e.g., 2,3]. The Ryugu samples collected by the Hayabusa2 spacecraft thus may have originated from different parts of the parent asteroid and experienced different thermal histories. We reported that Ryugu's secondary minerals such as dolomite and magnetite formed at 37±10°C, ~5.2 Ma after the formation of the Solar System based on oxygen and Mn-Cr isotope systematics of the sample A0058 collected from the first touch-down site on Ryugu [4]. Here we report oxygen and Mn-Cr isotope systematics of secondary minerals found in a Ryugu sample, C0002, collected from the 2<sup>nd</sup> touch-down site.

In contrast to A0058-C1001 section, C0002-C1001 section is composed of different lithological units recognizable by differences in BSE contrast and elemental distributions in X-ray maps, including less-altered lithologies [e.g., 3,5]. Most lithologies are dominated by phyllosilicate matrices with sub-micron magnetite and sulfide grains. Larger grains (>10 μm) of magnetite, dolomite, and pyrrhotite are scattered throughout the major lithologies.

Figure 1 shows O-isotope compositions of dolomite, magnetite from the C0002 section, together with those from A0058-C1001. The O-isotope compositions of the dolomites are consistent with those in A0058, and are similar to the bulk Ryugu within uncertainty for their  $\Delta^{17}\text{O}$  values [4,6,7]. In contrast to the majority of magnetites in A0058 having  $\Delta^{17}\text{O}$  of ~ 0‰, all magnetites but one in C0002 have higher  $\Delta^{17}\text{O}$ , ~ 2–3‰ (see also [8]). Some magnetites with high  $\Delta^{17}\text{O}$  are included in overgrown dolomites with  $\Delta^{17}\text{O}$  of ~ 0‰, suggesting earlier formation of these magnetites than the dolomite. These observations suggest that O-isotope composition of aqueous fluid was  $\Delta^{17}\text{O} \sim +3\%$  before crystallization of dolomite and was  $\Delta^{17}\text{O} > +3\%$  at the beginning stage of aqueous alteration because olivine and pyroxene in Ryugu have lower  $\Delta^{17}\text{O}$  (–24 to –5 ‰) [3,9,10].

Using O-isotope thermometry [e.g., 11], the dolomite and magnetite pair in A0058 was used to estimate a temperature at which these minerals precipitated; their O-isotope compositions correspond to 37±10°C [4]. In C0002, a pair of dolomite and magnetite in the same lithology has identical  $\Delta^{17}\text{O}$ , ~+0.6‰. Assuming these grains were in O-isotope equilibrium with the same fluid, their difference in  $\delta^{18}\text{O}$ , 25.2±2.0‰, corresponds to 104±22°C.

Figure 2 shows Mn-Cr isotope systematics of dolomites in A0058-C1001, C0002-C1001, and Ivuna CI chondrite. Note we collected Mn-Cr isotope data from dolomites from which the O-isotope data were obtained. All <sup>53</sup>Cr excesses are well correlated with Mn-Cr ratios. The inferred initial <sup>53</sup>Mn/<sup>55</sup>Mn ratios are (2.55±0.35)×10<sup>-6</sup>, (3.78±0.34)×10<sup>-6</sup>, and (3.14±0.25)×10<sup>-6</sup> for A0058-C1001 [4], C0002-C1001 [this study], and Ivuna [4, this study], respectively. The initial <sup>53</sup>Mn/<sup>55</sup>Mn ratio we obtained from C0002 is consistent with that in [10] and that from bulk Mn-Cr data [12] within uncertainty. If we use the initial <sup>53</sup>Mn/<sup>55</sup>Mn ratio of the D'Orbigny angrite and the U-corrected Pb-Pb ages of D'Orbigny and CV CAIs [13–15], the initial <sup>53</sup>Mn/<sup>55</sup>Mn ratios for A0058 and C0002 suggest that dolomite precipitation occurred at 5.2 (+0.8/–0.7) Ma and 3.1 (+0.5/–0.5) Ma after the CV CAI formation, at ~40°C and ~100°C, respectively. These ages could be systematically changed ±million years due to inconsistencies in CAI ages and proposed initial <sup>53</sup>Mn/<sup>55</sup>Mn ratios of the Solar System [4 and references therein]. Other systematic changes may be introduced by inaccurate corrections of Mn/Cr sensitivity for dolomite by SIMS [4, 16–18]. Despite these systematic uncertainties, the relative age between the two isochrons is robust: 2.1±0.9 Ma. Therefore, during the aqueous alteration, one location in the Ryugu parent asteroid was at ~100°C. Then ~2 Ma later, possibly another location in the asteroid experienced ~40°C. These are new conditions to restrict thermal models of the Ryugu parent body. Thermal modeling to satisfy the conditions is in progress using methods in [19].

**References:** [1] Sugita S. et al. *Science*, 364, eaaw0422 (2019). [2] Hopp T. et al. *Science Adv.*, accepted. [3] Kawasaki N. et al. *Science Adv.*, in review. [4] Yokoyama T. et al. *Science*, 10.1126/science.abn7850 (2022) [5] Nakamura T. et al. *Science*, 10.1126/science.abn8671 (2022). [6] Tang H. et al. *Science Adv.*, in review. [7] Fujiya W. et al. this volume. [8] Kita N. T. et al. this volume. [9] Liu M.-C. et al. *Nature Astron.*, 10.1038/s41550-022-01762-4 (2022). [10] Nakamura E. et al. *Proc. Japan Acad. B.*, 98, 227–282. (2022). [11] Zheng Y.-F. *Geochem. J.*, 45, 341–354 (2011). [12] Yokoyama T. et al. 53<sup>rd</sup> LPSC abstract #1272 (2022). [13] Glavin D. P. et al. *MAPS*, 39, 693–700 (2004). [14] Brennecka G. A. and Wadhwa M. *PNAS*, 109, 9299–9303 (2012). [15] Connelly J. N. et al. *Science*, 338, 651–655 (2012) [16] Steel R. C. et al. *Geochim. Cosmochim. Acta*, 201, 245–259 (2017). [17] McCain K. A. et al. *J. Vac. Sci. Technol.*, 38, 044005 (2020). [18] Sugawara S. et al. this volume. [19] Fujiya W. et al. *ApJL*, 924:L16 (2022).

**The Hayabusa2-initial-analysis chemistry team:** T. Yokoyama, K. Nagashima, Y. Abe, J. Aléon, C.M.O'D. Alexander, S. Amari, Y. Amelin, K. Bajo, M. Bizzarro, A. Bouvier, R. W. Carlson, M. Chaussidon, B.-G. Choi, N. Dauphas, A.M. Davis, T. Di Rocco, W. Fujiya, R. Fukai, I. Gautam, M.K. Haba, Y. Hibiya, H. Hidaka, H. Homma, P. Hoppe, G.R. Huss, K. Ichida, T. Iizuka, T.R. Ireland, A. Ishikawa, M. Ito, S. Itoh, N. Kawasaki, N.T. Kita, K. Kitajima, T. Kleine, S. Komatani, A.N. Krot, M.-C. Liu, Yuki Masuda, K.D. McKeegan, M. Morita, K. Motomura, F. Moynier, I. Nakai, A. Nguyen, L. Nittler, M. Onose, A. Pack, C. Park, L. Piani, L. Qin, S.S. Russell, N. Sakamoto, M. Schönbächler, L. Tafla, H. Tang, K. Terada, Y. Terada, T. Usui, S. Wada, M. Wadhwa, R.J. Walker, K. Yamashita, Q.-Z. Yin, S. Yoneda, E.D. Young, H. Yui, A.-C. Zhang, H. Yurimoto.

**The Hayabusa2-initial-analysis core:** S. Tachibana, T. Nakamura, H. Naraoka, T. Noguchi, R. Okazaki, K. Sakamoto, H. Yabuta, H. Yurimoto, Y. Tsuda, S. Watanabe.

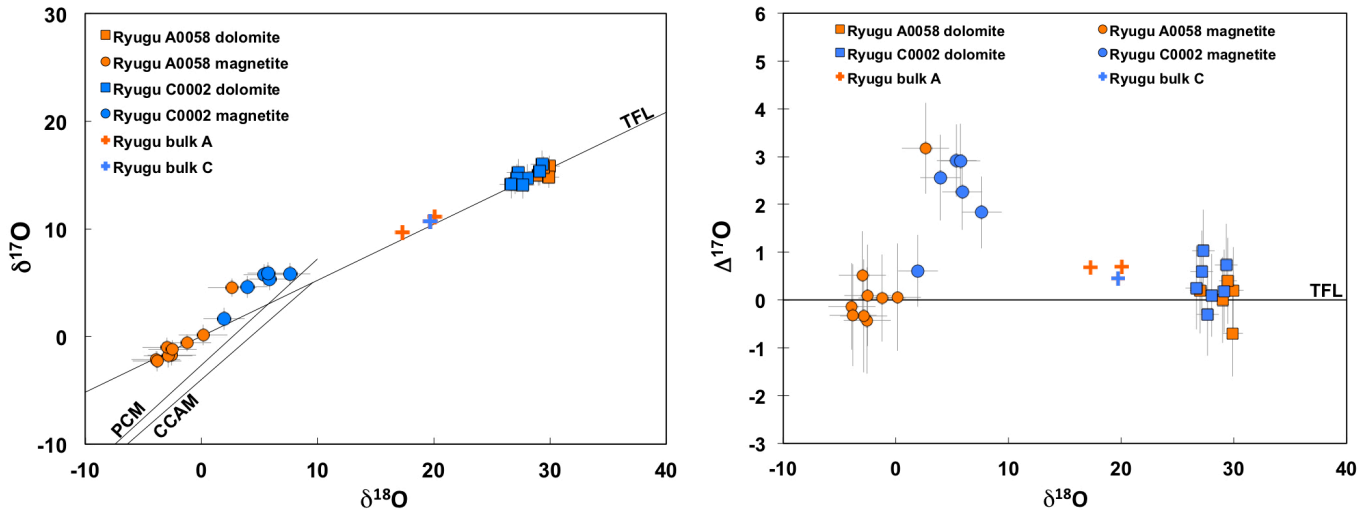


Fig. 1. Oxygen isotope compositions of dolomite and magnetite from Ryugu samples, A0058-C1001 [4] and C0002-C1001 [7, this study]. Also shown are bulk O-isotope data of A and C samples [4,6].

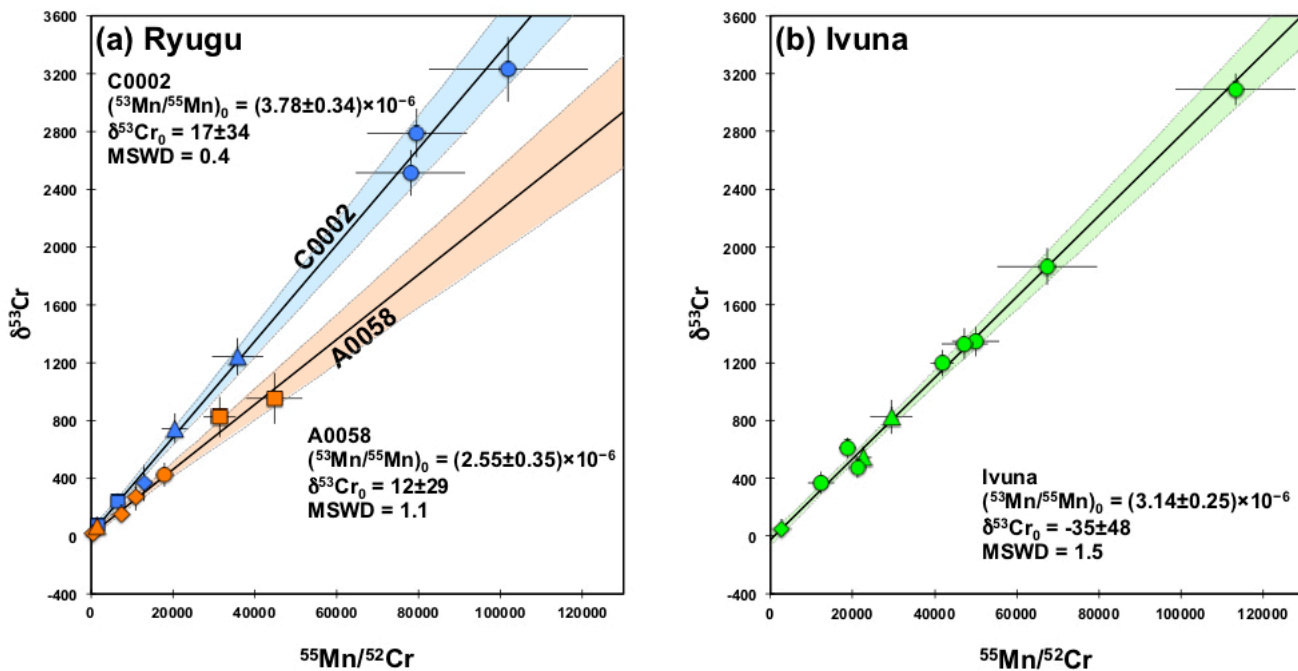


Fig. 2. Mn-Cr isotope systematics of dolomites from (a) Ryugu samples, A0058-C1001 [4] and C0002-C1001 [this study], and (b) Ivuna [4, this study]. Several dolomite grains were analyzed from each sample and they are shown as different symbols. Note data from dolomite grain HK2-#7 in Ivuna, shown as green circles were obtained in the two measurement sessions when we analyzed A0058-C1001 and C0002-C1001 samples and showed no differences in their initial  $^{53}\text{Mn}/^{55}\text{Mn}$  ratios.

# Elastic property of Ryugu samples collected at the second touch-down site

Keisuke Onodera<sup>1</sup>, Yuta Ino<sup>2,3</sup>, Satoshi Tanaka<sup>3</sup>, Taichi Kawamura<sup>4</sup>, Takuya Ishizaki<sup>3</sup>, Ryota Fukai<sup>3</sup>, Rei Kanemaru<sup>3</sup>, Takahiro Iwata<sup>3</sup>, Tomoki Nakamura<sup>5</sup>, HAYABUSA2 initial sample analysis team

<sup>1</sup>*Earthquake Research Institute, The University of Tokyo*

<sup>2</sup>*Kwansei Gakuin University*

<sup>3</sup>*Institute of Space Astronautical Science, Japan Aerospace Exploration Agency*

<sup>4</sup>*Institut de Physique du Globe de Paris, Université Paris Cité*

<sup>5</sup>*Department of Earth Sciences, Tohoku University*

## Introduction

Since the HAYABUSA2's successful return from the 6 years of space journey on December 5<sup>th</sup> 2020, many analyses of the collected samples have been conducted (e.g., [1]-[4]). Those studies help us better understand the ancient history of the solar system as well as the Ryugu's characteristics and its origin.

According to the initial analysis [1]-[3], it turned out that Ryugu showed high similarity to CI chondrites (e.g., Ivuna, Orgueil) from the petrological or mineralogical aspect. For example, Visible-Near infrared reflectance spectra of Ryugu samples show a sharp absorption at 2.72  $\mu\text{m}$  – consistent with the remote sensing observation [5] – and weak absorptions at 3.4 and 3.95  $\mu\text{m}$  as seen in CI chondrites. These observations provide us with chemical features, allowing us to interpret how these particles were formed under what kind of environment.

In addition to chemical aspects, physical properties such as density, porosity, and rigidity are also of great importance. Especially, rigidity is one of the paramount parameters to constrain the formation process from the catastrophic impact to re-accumulation to make a rubble pile body [4]. Also, the elastic behavior like seismic wave propagation is closely related to the asteroid's surface evolution (e.g., seismic shaking).

In this study, through the measurement of seismic wave velocity, we are trying to provide a detailed description on elastic properties such as seismic wave velocity, Young's modulus, and attenuation quality factor. Moreover, by comparing the derived parameters with those for other carbonaceous chondrites, we discuss which type is the most similar to Ryugu from the viewpoint of elastic property.

## Samples used for measurements

For the measurements, C0002-No3 and No4 were allocated to us. Both particles are mm scale with a thickness of 0.5 – 1.0 mm, cut out of one of the largest samples collected at the second touch-down site. Figure 1 shows the micrographs of the respective particles. Note that the C0002-No4 was broken into two pieces over the course of the physical property measurements [4], and we measured their seismic waves individually.

## Seismic wave velocity measurement and estimation of Young's modulus

We adopted the pulse transmission method [6] to measure P and S wave velocities. The experimental setting is shown in Figure 2, where a sample is sandwiched with two transducers placed on an electronic scale. This kind of setting allows us to measure the wave velocity monitoring the loading simultaneously. The principle is to transmit a pulse from one side transducer to another side for two settings: (i) transducers without sample, (ii) transducers with a sample interposed. Then, we can obtain the time delay by comparing two signals (Figure 3). Since the thickness and density of each sample are known, the seismic wave velocity and Young's modulus can be obtained in the end. As a result, we obtained  $V_p=1.9 - 2.3$  km/s,  $V_s=1.2 - 1.4$  km/s, and 6.2 – 8.6 GPa for Young's

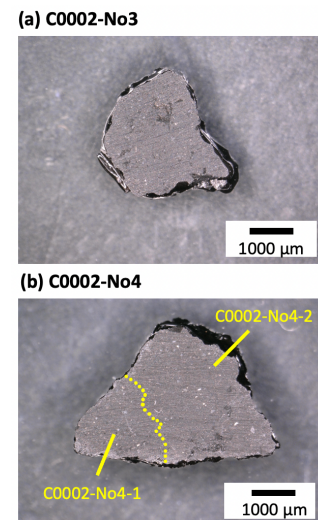


Figure 1. Micrographs of Ryugu sample (a: C0002-No3, b: C0002-No4). For the measurements, we used the divided pieces of C0004-No4 (1&2).

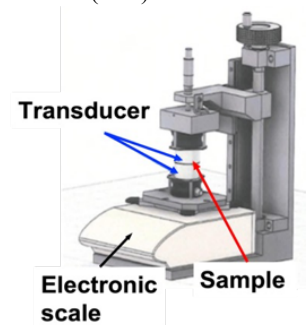


Figure 2. Schematic illustration of the experimental setting.

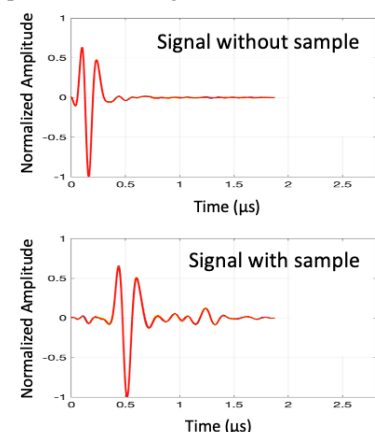


Figure 3. Transmitted signal without sample (top) and with sample (bottom). Time delay between them gives seismic wave velocity.

modulus under 1 MPa loading (Table 1). While Nakamura et al. [4] reported the average values of these samples, this presentation will show the individual results. Moreover, we discuss whether Ryugu is similar to CI chondrites also from elastic property through the comparison of our results with those for various carbonaceous chondrites.

Table 1. P- and S-wave velocities and Young's modulus for each sample

Sample name	$V_p$ (km/s)	$V_s$ (km/s)	Young's modulus (GPa)
C0002-No3	$2.25 \pm 0.01$	$1.42 \pm 0.15$	$8.58 \pm 3.17$
C0002-No4-1	$1.94 \pm 0.01$	$1.20 \pm 0.01$	$6.24 \pm 2.80$
C0002-No4-2	$1.96 \pm 0.01$	$1.32 \pm 0.07$	$6.88 \pm 2.34$

## References

- [1] Yada et al. (2022), Preliminary analysis of the Hayabusa2 samples returned from C-type asteroid Ryugu, *Nat Astron*, 6, 214–220, <https://doi.org/10.1038/s41550-021-01550-6>.
- [2] Yokoyama et al. (2022), Samples returned from the asteroid Ryugu are similar to Ivuna-type carbonaceous meteorites, *Science*, 10.1126/science.abn7850.
- [3] Ito et al. (2022), A pristine record of outer Solar System materials from asteroid Ryugu's returned sample, *Nat Astron*, <https://doi.org/10.1038/s41550-022-01745-5>.
- [4] Nakamura et al. (2022), Formation and evolution of carbonaceous asteroid Ryugu: Direct evidence from returned samples, *Science*, 10.1126/science.abn8671.
- [5] Kitazato et al. (2019), Surface composition of asteroid 162173 Ryugu as observed by the Hayabusa2 NIRS3 instrument. *Science*, 364, 272–275.
- [6] Blair (1996), Estimates of seismic attenuation using vibrational resonance and pulse transmission in four large blocks of rock, *GJI*, 126, 135-146.

## Slickenside as a record of shock metamorphism on asteroid Ryugu

M. Miyahara<sup>1</sup>, T. Noguchi<sup>2</sup>, T. Matsumoto<sup>2</sup>, N. Tomioka<sup>3</sup>, A. Miyake<sup>2</sup>, Y. Igami<sup>2</sup>, Y. Seto<sup>4</sup>, T. Nakamura<sup>5</sup>, H. Yurimoto<sup>6</sup>, R. Okazaki<sup>7</sup>, H. Yabuta<sup>1</sup>, H. Naraoka<sup>7</sup>, S. Tachibana<sup>8</sup>, S. Watanabe<sup>9</sup>, Y. Tsuda<sup>10</sup>, and the Hayabusa2 Initial Analysis “Sand” Team  
<sup>1</sup>Hiroshima Univ., Japan; <sup>2</sup>Kyoto Univ., Japan; <sup>3</sup>JAMSTEC, Japan; <sup>4</sup>Osaka Metropolitan Univ., Japan; <sup>5</sup>Tohoku Univ., Japan; <sup>6</sup>Hokkaido Univ., Japan; <sup>7</sup>Kyushu Univ., Japan; <sup>8</sup>Univ. of Tokyo, Japan; <sup>9</sup>Nagoya Univ., Japan.; <sup>10</sup>JAXA/ISAS, Japan.

**Introduction:** An asteroid is formed and evolved by repeated collisions. The Hayabusa2 spacecraft shows that boulders with layered structures occur on the asteroid Ryugu (*I*). The layered structure can be regarded as parallel cracks, which is one of the representative features related to shock metamorphism. Evidence of shock metamorphism is found in some polished Ryugu grains (C0055) (2). However, evidence of shock metamorphism has not been found on the surface of Ryugu grains. In the present study, we scrutinize the surface morphology of several Ryugu grains to find features of shock metamorphism.

**Samples and experimental methods:** Numerous small Ryugu grains, ~100  $\mu\text{m}$  across on average, were allocated to the M-P F sub-team. Several grains from the chamber A (surface particles collected by the first touchdown) were attached on a gold (Au) plate (sample plate number: AP 042) with small amounts of epoxy glue in an  $\text{N}_2$  filled glove box for surface morphology observation. The surface morphology of grains without any coating was observed by JEOL JSM-7100F and Hitachi S-5200 field emission gun scanning electron microscopes (FEG-SEM) at Tohoku Univ. and Hiroshima Univ., respectively. Some portions in the grains were excavated and processed to be ultrathin foils by a Hitachi SMI4050 focused ion beam (FIB) system at Kochi Institute for Core Sample Research, JAMSTEC after coating with osmium and carbon. The ultrathin foils were examined by a JEOL JEM-2100F transmission electron microscope (TEM) equipped with an energy dispersive spectrometer (EDS) at Tohoku Univ. Chemical compositions were measured by EDS under scanning TEM (STEM) mode.

**Results and discussion:** More than 24 grains adhered on the sample plate AP 042 were observed by secondary electron (SE) imaging (at a low accelerating voltage of 3.0–5.0 kV) to scrutinize the surface morphology. Some grains were broken into finer grains when grains were put on an Au plate, follows that fresh surface appeared newly. Most grains had a bumped or rough surface, and some grains had evidence of space weathering (3). On the other hand, two grains had a smooth surface on one side of the grain (Fig. 1). The smooth surface is not a single crystal surface. An obscure liner texture was observed on the smooth surface of one grain. An ultrathin foil was prepared from the smooth surface with a liner structure to observe its cross-section. The smooth surface looks like a weathering vein consisting of carbonate or iron-hydro/oxide minerals which are found in some carbonaceous chondrites. However, X-ray elemental maps indicated that there is no distinct difference in chemical compositions near the smooth surface. Bright-field (BF)-TEM images showed that the ultrathin foil consists mainly of fibrous phyllosilicates (saponite and serpentine) assemblage embedding small amounts of iron-sulfide and iron-oxide grains. The fibrous phyllosilicate assemblage is porous, and pores are filled with organic matter. These mineralogical features are like the Ryugu grains investigated in other works (3, 4). However, there is a distinct difference: the fibrous phyllosilicates assemblage near the smooth surface is compacted and the compaction degree increases toward the smooth surface. Lattice fringes corresponding to phyllosilicates become obscure with approaching the smooth surface, indicative of vitrification or dehydration. A ~200 nm layer from the smooth surface is heavily compacted, where the (001) basal planes of fibrous phyllosilicates are sub-parallel to the smooth surface. The smooth surface with a liner texture is a characteristic feature of a slickenside, which is found in terrestrial fault rocks and shatter cones around impact craters (5). The slickenside is formed by friction

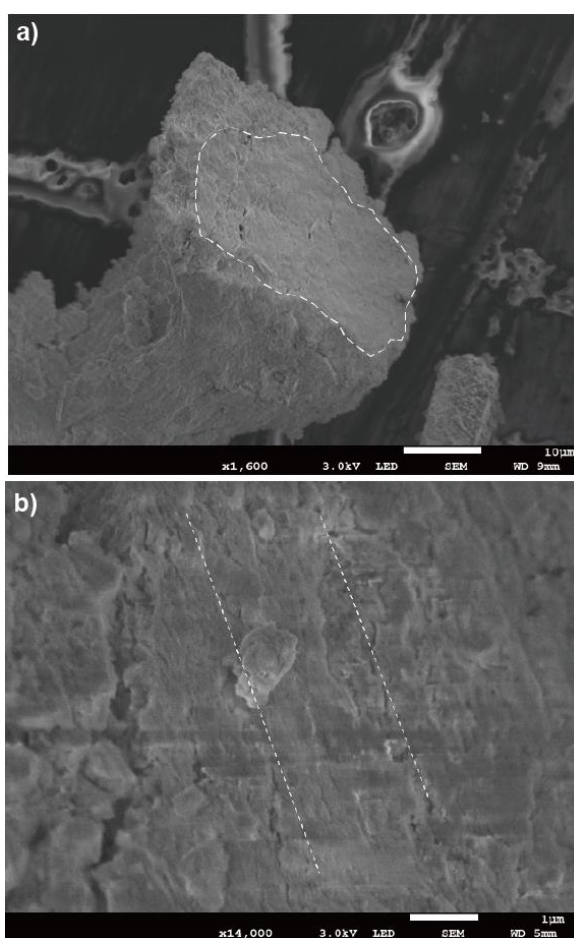


Figure 1. SE images. a) A grain with a smooth surface (dashed line) and b) a high-magnification image of the smooth surface with a liner structure (dotted line). Horizontal parallel stripes are artifact because of electron charge-up.

between rocks along the two sides of a fault. Hence, we propose that the smooth surfaces appearing on some Ryugu grains are the record of shock-induced shear deformation that occurred on the asteroid Ryugu. No evidence of decomposition is found in fibrous phyllosilicates near the smooth surface of Ryugu grains. This suggests that friction heating temperature is below the decomposition temperature of phyllosilicates ( $< \sim 700$  °C) (6). A shock-melt vein is also formed by friction heating along a faulting zone in shocked meteorites (7). Such a melting texture is not observed in Ryugu grains. Ryugu's grains with slickensides do not adhere well to each other because shock-induced melting and subsequent quenching did not occur. Therefore, grains with slickensides can be easily detached from each other during fall into the earth. In addition, a slickenside is too thin to survive from atmospheric entry heating or terrestrial weathering. So, a slickenside could not be found in a meteorite.

## References

- (1) S. Tachibana *et al.*, Pebbles and sand on asteroid (162173) Ryugu: In situ observation and particles returned to Earth. *Science* **375**, 1011–1016 (2022).
- (2) T. Nakamura *et al.*, Formation and evolution of carbonaceous asteroid Ryugu: Direct evidence from returned samples. *Science* <https://doi.org/10.1126/science.abn8671> (2022)
- (3) T. Noguchi *et al.*, Mineralogy and space weathering of fine fraction recovered from asteroid (162173) Ryugu. the 53<sup>rd</sup> Lunar and Planetary Science Conference, Houston, 1747.pdf, 2022.
- (4) T. Matsumoto *et al.*, Mineralogical analysis of various lithologies in coarse Ryugu samples using transmission electron microscopy the 53<sup>rd</sup> Lunar and Planetary Science Conference, Houston, 1344.pdf, 2022.
- (5) D. Baratoux, W. U. Reimold, The current state of knowledge about shatter cones: Introduction to the special issue. *Meteorit. Planet. Sci.* **51**, 1389–1434 (2016).
- (6) J. N. Weber, R. T. Greer, Dehydration of serpentine: Heat of reaction and reaction kinetics at  $P_{H_2O}=1$  atm. *Am. Min.* **50**, 450–464 (1965).
- (7) P. Gillet, A. E. Goresy, Shock events in the Solar System: The message from minerals in terrestrial planets and asteroids. *AREPS* **41**, 257–285 (2013).

# Spectral variations in serpentine and saponite 2.7 $\mu\text{m}$ band due to heating under vacuum.

S. Sidhu<sup>1</sup>, D. Applin<sup>1</sup>, E. A. Cloutis<sup>1</sup>, and A. Maturilli<sup>2</sup>

<sup>1</sup>Centre for Terrestrial and Planetary Exploration, University of Winnipeg, Winnipeg, Manitoba, R3B 2E9, Canada.

<sup>2</sup>Institute for Planetary Research, German Aerospace Center DLR, Rutherfordstr. 2, 12489 Berlin, Germany

**Introduction:** Carbonaceous chondrites (CCs) are scientifically significant as they present a window into the early Solar System. Many classes of meteorites are considered primitive and provide an opportunity to study early solar system chemistry [1]. Carbonaceous chondrites in the sub-group CM2 likely underwent aqueous alteration to various degrees, resulting in formation of alteration minerals such as phyllosilicates [2]. Here we present a heating experiment conducted on two phyllosilicates and a simple two-component phyllosilicate + carbonaceous phase spectral analogue powder created at the Centre for Terrestrial and Planetary Exploration (C-TAPE) at the University of Winnipeg, Canada.

**Methods:** Samples of saponite (C-TAPE ID: SAP104), serpentine (C-TAPE ID: ASB267), and CC spectral analogue, created in-house, MUD008 (C-TAPE ID) were heated up to 900°C under vacuum ( $\sim 0.07$  mbar) in 100°C increments for 1 hour at each temperature increment. Heating was conducted using an induction heating system in the external emissivity chamber at the Planetary Spectroscopy Lab (PSL) at DLR, Berlin. Samples were allowed to cool in the vacuum chamber and then removed from vacuum and transferred to the spectrometer. The sample was then evacuated down to  $\sim 0.1$  mbar prior to the spectral measurements. Data were collected using a Bruker Vertex 80v FTIR spectrometer using the Bruker A513 bi-directional reflectance accessory. Reflectance data were collected over the VISNIR (0.4 – 1.1  $\mu\text{m}$ ) and MIR (1.1 – 20  $\mu\text{m}$ ), however for the purposes of this report, only results up to 5  $\mu\text{m}$  are discussed and displayed in the figures below. A new sample was used for each temperature increment.

**Results:** Progressive heating of SAP104 generally displays a decrease in reflectance values as temperatures increase in the VISNIR (0.4 – 1.1  $\mu\text{m}$ ). In the MIR (1.1 – 20  $\mu\text{m}$ ), the spectra brighten slightly up to 300°C, after which the reflectance starts to decrease. The H<sub>2</sub>O absorption feature  $\sim 2.7$   $\mu\text{m}$  decreases in depth with increasing temperature, displaying qualitatively the deepest band at the room temperature observation and the shallowest band at 900°C (see Figure 1).

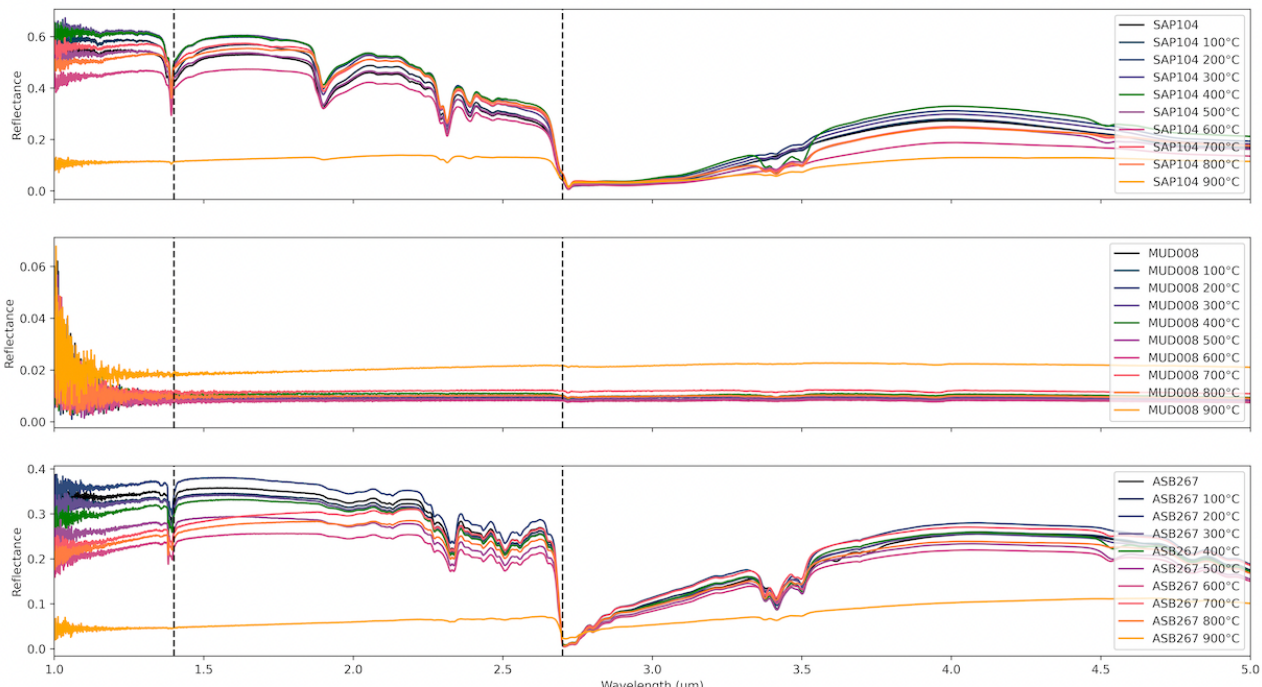


Figure 1: MIR (1-5  $\mu\text{m}$ ) reflectance spectra of SAP104 (top), MUD008 (middle), and ASB267 (bottom) heated up to 900°C for 1 hour at each 100°C increment under vacuum.

ASB267 displays a similar trend upon heating as SAP104's spectra regarding reflectance values: generally, decreases in the VISNIR and slightly increases then decreases in the MIR with increasing temperature. Also, similar to SAP104, the  $\sim 2.7$   $\mu\text{m}$  absorption feature systematically decreases in depth as a function of increasing temperature.

MUD008 (90 wt.% SAP105 saponite, <45  $\mu\text{m}$  grain size + 10 wt.% LCA101 carbon lampblack, <0.021  $\mu\text{m}$  grain size) gets spectrally brighter as a result of heating in both the VISNIR and the MIR, which may be due to the volatilization of carbon. MUD008 displays a slight  $\sim 2.7 \mu\text{m}$  feature which gets shallower with increasing temperature, consistent with the spectra of SAP104 and ASB267 (serpentine).

Other OH/H<sub>2</sub>O related features  $\sim 1.4$  and  $1.9 \mu\text{m}$  are observable in both SAP104 and ASB267 spectra. After exposure to high temperatures, these absorption features also decrease in depth, consistent with the  $\sim 2.7 \mu\text{m}$  feature. Metal-OH features near  $\sim 2.3 \mu\text{m}$  are also visible in both phyllosilicate samples. By  $900^\circ\text{C}$ , the absorption features are drastically reduced in depth.

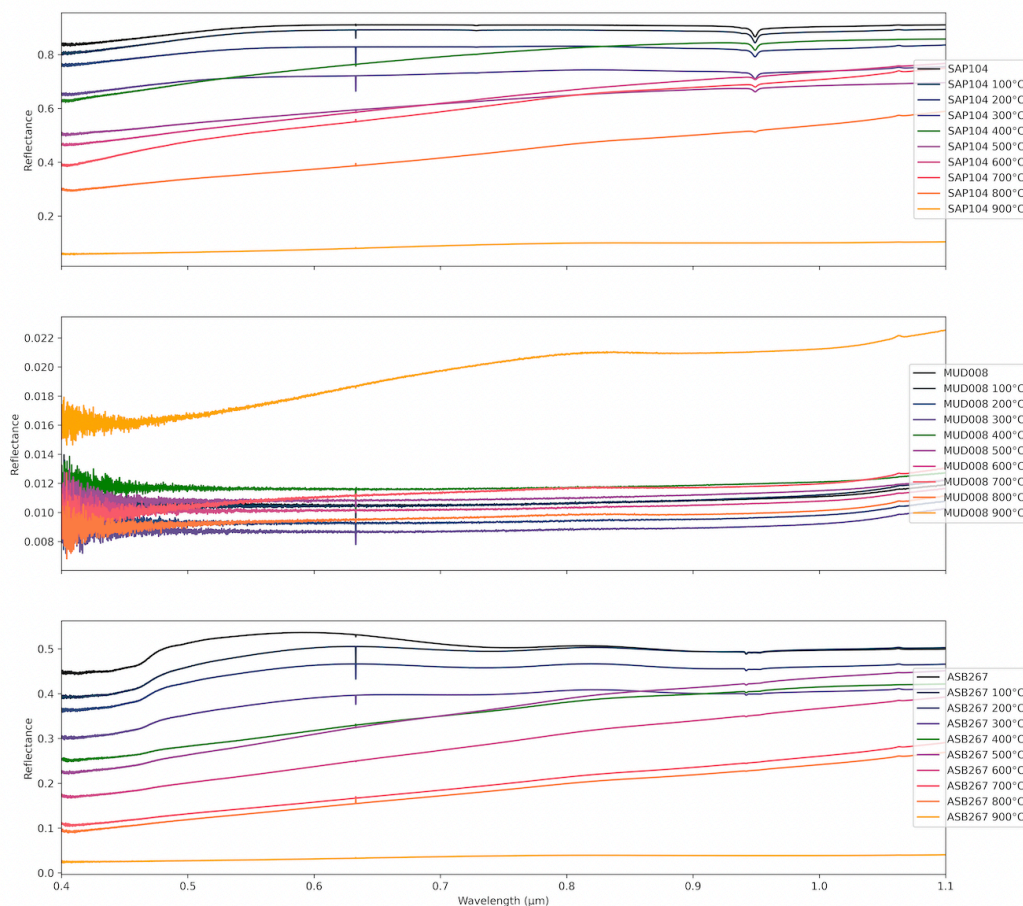


Figure 2: VISNIR (0.4 – 1.1  $\mu\text{m}$ ) reflectance spectra of SAP104 <45  $\mu\text{m}$  (top), MUD008 <45  $\mu\text{m}$  (middle), and ASB267 <45  $\mu\text{m}$  (bottom) heated under vacuum up to  $900^\circ\text{C}$  in  $100^\circ\text{C}$  increments. Spectral artifact at  $\sim 0.64 \mu\text{m}$ .

**Discussion:** Our spectra show that several OH/H<sub>2</sub>O absorption features at  $\sim 1.4$ ,  $\sim 1.9$ , and  $\sim 2.7 \mu\text{m}$  become shallower with increasing temperature in SAP104 and ASB267. In addition, the Mg-OH features near  $\sim 2.3 \mu\text{m}$  also decrease in strength with increasing temperature in both saponite and serpentine samples. These results are part of an on-going study investigating the spectral and mineralogical variations in saponite, serpentine and MUD008 due to thermal exposure under vacuum conditions. Future work includes collecting X-ray diffraction data on the heated samples presented in this study and relate any mineralogical changes to the spectral variations observed.

**Acknowledgements:** This project has received funding from the European Union's Horizon 2020 research and innovation programme under grant agreement No 871149. Thanks are due to the Canadian Space Agency (CSA), the Natural Sciences and Engineering Research Council of Canada (NSERC), the Canadian Foundation for Innovation (CFI), the Manitoba Research Innovation Fund (MRIF) and the University of Winnipeg for supporting this study.

## References

- [1] McSween, H. 1979. *Reviews of Geophysics & Space Physics* 17:5. [2] Rubin, A. E. et al. 2007. *Geochimica et Cosmochimica Acta* 71:9.

# Mn/Cr relative sensitivity factors of SIMS determined for synthetic Mn-, Cr-, and Fe-bearing dolomites

Shingo Sugawara<sup>1</sup>, Wataru Fujiya<sup>1</sup>, Akira Yamaguchi<sup>2</sup>, Ko Hashizume<sup>1</sup>

<sup>1</sup>Ibaraki University

<sup>2</sup>National Institute of Polar Research

Dolomite [CaMg(CO<sub>3</sub>)<sub>2</sub>] is a carbonate mineral commonly found in aqueously altered carbonaceous chondrites and contains some amounts of Mn and Fe. Dolomite in meteorites formed in the early solar system and incorporated a short-lived radionuclide <sup>53</sup>Mn that decays to <sup>53</sup>Cr with a half-life of 3.7 million years [1]. Thus, the timescale of aqueous alteration and the formation age of parent bodies can be constrained by <sup>53</sup>Mn-<sup>53</sup>Cr dating of meteoritic dolomite.

The Mn-Cr dating of dolomite has commonly been performed using secondary ion mass spectrometry (SIMS). For SIMS analyses, the relative sensitivity factor (RSF) defined as a Mn<sup>+</sup>/Cr<sup>+</sup> ion intensity ratio divided by a Mn/Cr elemental ratio must be evaluated using a standard material with the same composition as the meteoritic carbonate to be analyzed to correct the matrix effect. However, because carbonates in the natural environment contain little Cr, it is challenging to utilize a proper Cr-bearing dolomite standard, and therefore, the previously reported Mn-Cr ages of meteoritic dolomite may have systematic uncertainties. To overcome this problem, the synthesis of Mn- and Cr-bearing dolomite has been attempted [8,9], although dolomite crystallization proceeds only under hydrothermal conditions, making it difficult to incorporate Cr. Alternatively, Mn- and Cr-bearing calcite [CaCO<sub>3</sub>] [10], which can be synthesized in aqueous solution at room temperature, has been used [2-5], but the RSFs of calcite and dolomite may be different. Recently, natural dolomite to which Cr ions were implanted was produced as a Cr-bearing dolomite standard [11,12]. However, the depth of the implantation was within 1 μm from the sample surface, and thus, the analytical conditions of this standard and meteoritic dolomite were much different, which may lead a systematic error on the obtained Mn-Cr ages.

In this work, we synthesized Mn-, Cr-, and Fe-bearing dolomites via amorphous carbonates. Amorphous calcium carbonate (ACC), which can incorporate large amounts of incompatible elements for crystal phases, crystallizes into calcite by heating [e.g., 13]. Applying this method, we synthesized Mn-, Cr-, and Fe-bearing dolomites via amorphous calcium magnesium carbonate (ACMC) with FeO contents of (i) 0 wt%, (ii) 0.95 wt%, and (iii) 3.17 wt%. Also, we synthesized Mn- and Cr-bearing calcite from ACC for comparison with previous studies [10].

We produced ACMCs by mixing a 0.2 M Na<sub>2</sub>CO<sub>3</sub> solution and a 0.2 M (Mg, Ca, Cr, Mn, Fe) Cl<sub>2</sub> solution. The ACMCs were dehydrated at 270-300 °C and crystallized to dolomite by heating at 310-420 °C under a 1-22 bar CO<sub>2</sub> atmosphere. The heated samples were washed with ultrapure water and dried in a vacuum desiccator. The run products were identified as single-phase dolomite by powder X-ray diffraction (XRD). We observed the dolomites with a field emission scanning electron microscope (FE-SEM) and found that they were from several 10s nanometer- to submicron-sized particles. Also, a Mn-, and Cr-bearing calcite was synthesized via ACC [13]. The Mn-, Cr-, and Fe-bearing dolomite and Mn- and Cr-bearing calcite particles were separately put in a tungsten carbide piston cylinder and pressed using a hydraulic press to produce pellets. These pellets were embedded in resin, and their surfaces were polished and then coated with carbon. Electron probe micro analysis confirmed that the <sup>55</sup>Mn/<sup>52</sup>Cr ratios of the dolomites were (i) 1.32 ± 0.02 (2SE, n = 185), (ii) 5.46 ± 0.14 (2SE, n = 391), and (iii) 2.70 ± 0.06 (2SE, n = 220), and that of the calcite was 0.86 ± 0.01 (2SE, n = 200).

Then, we analyzed the synthesized carbonates and a natural olivine from San Carlos using SIMS. Secondary ions of <sup>43,44</sup>Ca<sup>+</sup>, <sup>52,53</sup>Cr<sup>+</sup>, <sup>55</sup>Mn<sup>+</sup>, and <sup>57</sup>Fe<sup>+</sup> were produced with a ~1 nA O<sup>-</sup> primary ion beam focused to ~10 μm in diameter. The RSFs of olivine and calcite were 0.93 and ~0.75, respectively, consistent with previous studies [2-5, 10] (Fig. 1). We found that the RSFs of Fe-bearing dolomites increase with their FeO contents from ~0.81 to ~1.00, which is also consistent with the previous study [12] (Fig. 2). The observed variation in the RSFs between Fe-bearing dolomites and calcite could result in a systematic error on the ages of meteoritic dolomites by 1.6 Myr. We noted, however, that the reproducibility was worse when we used a primary ion beam with a lower intensity of 150 pA, probably due to the influence of the surface topography. This indicates that it is important to keep analytical conditions the same between the standard and meteoritic dolomites.

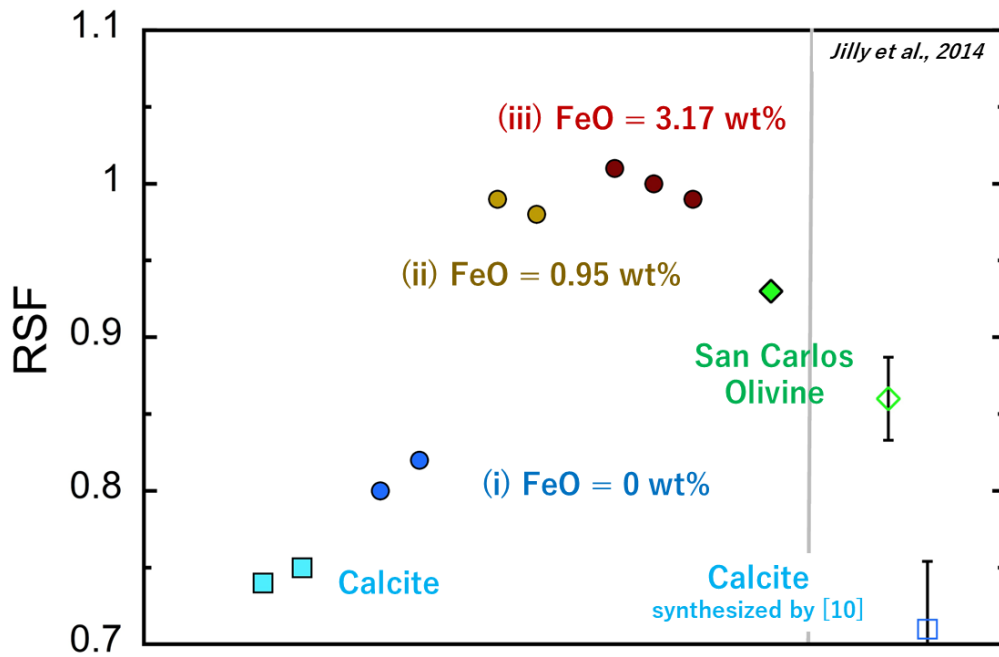


Fig.1. The relative sensitivity factors [RSF =  $(^{55}\text{Mn}/^{52}\text{Cr})_{\text{SIMS}}/(^{55}\text{Mn}/^{52}\text{Cr})_{\text{EPMA}}$ ] of synthetic dolomites, synthetic calcite, and San Carlos Olivine. RSFs obtained by Jilly et al. [4] are shown by open symbols for comparison.

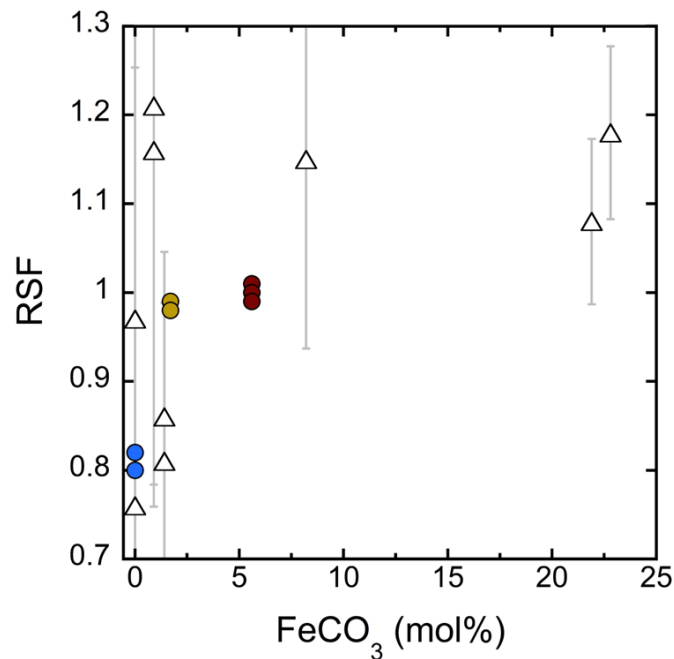


Fig. 2. The RSFs of synthetic dolomites as a function of Fe contents. RSFs obtained by McCain et al. [12] are shown by open symbols for comparison.

## References

- [1] Honda M. and Imamura M. 1971. Phys. Rev. C 4, 1182–1188. [2] Fujiya W. et al. 2012. Nat. Commun. 3, 627. [3] Fujiya W. et al. 2013. Earth Planet. Sci. Lett. 362, 130–142. [4] Jilly C. et al. 2014. Meteorit. Planet. Sci. 49, 2104–2117. [5] Jilly C. et al. 2017. Geochim. Cosmochim. Acta 201, 224–244. [6] Yokoyama T. et al. 2022. Science eabn7850. [7] Nakamura E. et al. 2022. Proc. Jpn. Acad., Ser. B 98, 227–282. [8] Ichimura K. and Sugiura N. 2015. Abstract #1795 LPSC. [9] Donohue P. et al. 2019. Abstract #1949 LPSC. [10] Sugiura N. et al. 2010. Geochem. J. 44, 11–16. [11] Steele R. et al. 2017. Geochim. Cosmochim. Acta 201, 245–259. [12] McCain K. et al. 2020. J. Vac. Sci. Technol. B38, 044005 [13] Miyajima Y. et al. 2020. Geostand. Geoanal. Res. 45, 189–205.

# Winchcombe CM2 meteorite fall 2021 – first results of systematic LASER Raman Spectroscopy

V.H.Hoffmann<sup>1</sup>, M. Kaliwoda<sup>1,2</sup>, M. Junge<sup>1,2</sup>, W.W. Schmahl<sup>1,2</sup>

<sup>1</sup>Faculty of Geosciences, Department of Geo- and Environmental Sciences, University of Munich;

<sup>2</sup>Mineralogical State Collection Munich (MSM-SNSB), Munich, Germany

In our (online) poster we will report the first results of detailed studies by 2/3 D digital microscopy and high resolution LASER Raman Spectroscopy on the Winchcombe CM2 meteorite. This project is part of our ongoing investigations on the mineralogy and phase composition on selected and recent falls of carbonaceous chondrites [1,2 and refs. herein]. Scientific background of these studies are preinvestigations and necessary technical/methodological developments in the fore-field of the planned projects on Hayabusa 2 (asteroid Ryugu) and Osiris Rex (asteroid Bennu) returned materials [3,4].

## Introduction

The Winchcombe meteorite fireball and fall from 28th february 2021 was the first reported meteorite fall of a carbonaceous chondrite in the UK [5-10]. The next day after the fireball the first finds were made in the private yard of local people (Wilcock family) followed by a number of further finds in the Winchcombe area (total reported mass about 602gr). Most of the finds were not influenced by any rains. We obtained fragment(s) of the first find made by the Wilcock family for our investigations.

## Samples

Figure 1a: Our sample(s), 3D digital microscopy: fragment(s) of the Wilcock find, heavily brecciated, relicts of chondrules and CAI; (b) Large Olivine particle - near forsterite in composition - in the very fine grained phyllosilicate (serpentine) matrix. (c) Calcite bearing well structured CAI.



Fig 1a.



Fig. 1b.



Fig. 1c.

## Methods, techniques

The (surface) morphology and mineralogy of the samples was pre-investigated by digital microscopy followed by detailed and systematic investigations with LASER Raman Spectroscopy [see 11,12 for details]. All Raman experiments have been performed without further preparation (only cutting) in order to avoid any unwanted effects (e.g. alterations). The obtained results should be representative because we did a large number of mappings in different scales on matrix and further components/clasts. We used the 532 nm LASER, Raman shifts were detected between 50-2500 (4500 for water content)  $\text{cm}^{-1}$  with a precision of  $\pm 1-2 \text{ cm}^{-1}$ , and magnifications of 100-1000x (long distance lenses only), and a lateral resolution of 0.1  $\mu\text{m}$ . Large maps up to 15x15 points in 2D/3D at high resolution allowed to also detect accessory phases / submicron particles and inclusions. Acquisition times of 1-3 sec and accumulation numbers of up to 5 have been used which allowed to obtain large numbers of Raman spectra in short times within the high resolution mappings, and therefore the results should be representative. Si and graphite standards were used for calibration measures, in most cases we applied a 6th degree polynomial for background subtraction.

## Results

The matrix of Winchcombe is dominated by phases of the serpentine mineral group which is a common feature of the CM chondrites and also of C1-C2 ungrouped CC such as Flensburg, Tarda or Tagish Lake [5]. On many matrix spots and different clasts the serpentine group member cronstedtite could be detected, generally intimately intergrown with the iron sulfide tochilinite (TCI).

Summarizing, the following phases and components could be found in our preliminary studies:

- Serpentine group members (main matrix component)
- Cronstedtite / tochilinite aggregates (CTI)
- Troilite, pyrrhotite?
- Orthopyroxene (OPX)
- Olivine (near forsterite)

- Tephroite – like phase (as in Aguas Zarcas)
- Carbon phases (no or poor crystallinity)
- CAI, calcite bearing
- A significant H<sub>2</sub>O content, more details elsewhere

We could not find any effects or influence of terrestrial alteration which confirms the high quality of the material. Further Raman experiments will focus on the minor / accessory phases, the chondrule components and on CAI. Summarizing, the found phase composition of our Winchcombe sample reflects the typical composition of a CM2 carbonaceous chondrite, with one exception – the tephroite like phase.

To perform successful LASER Raman spectroscopy experiments on carbonaceous chondrites, (in our recent projects on the Mukundpura, Flensburg, Tarda, Kolang, Aguas Zarcas and here Winchcombe meteorite falls) requires the design of a highly sophisticated experimental setup in order to avoid or at least minimize alteration effects already during the measurements on the one hand and to guarantee a reasonable signal/noise relationship on the other. Therefore we decided to investigate only naturally broken unprepared sample materials whenever possible. The representativity of the data obtained on the available sample material was also topic of our studies: large sets of high resolution mappings in 2D/3D can help to overcome the problem of tiny samples / fragments. Our main interests were on optimizing and fine tuning our experimental setup. So the series of recent meteorite falls which produced a new set of primitive carbonaceous chondrites provided us directly with unique fresh analogue materials for Hayabusa 2 (Ryugu) and Osiris Rex (Bennu) asteroidal samples in our laboratories.

Figure 2: Representative Raman spectra as obtained on our Winchcombe sample: (a) Olivine particle – near forsterite in composition and a significant concentration of non-crystalline carbon phases; (b) OPX (chondrule?) and indications for water in the matrix (Raman shift > 3000 cm<sup>-1</sup>); (c) Raman spectrum of a tephroite – like olivine group phase which we also could find for example in Aguas Zarcas (CM2). A tephroite like phase was not reported to our best knowledge from CM meteorites.

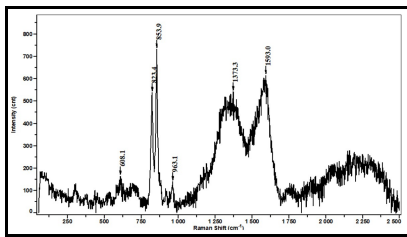


Fig. 2a.

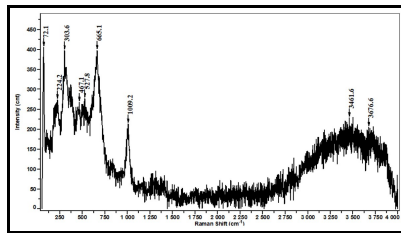


Fig. 2b.

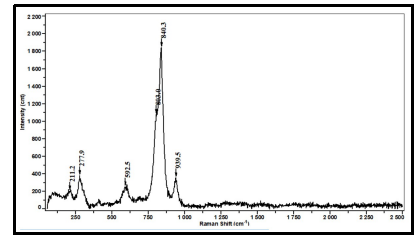


Fig. 2c.

## References

- [1] Hoffmann V.H. et al., 2021. 8th ISAS Symp. Solar System Mater. (Hayabusa 2021).
- [2] Hoffmann V.H., Kaliwoda M., Junge M., Schmahl W.W., 2022. LPSC conference, iposter, # 2231.
- [3] <https://www.hayabusa2.jaxa.jp>
- [4] <https://www.nasa.gov/osiris-rex>.
- [5] Meteoritical Bulletin: [www.lpi.usra.edu/meteor/metbull](http://www.lpi.usra.edu/meteor/metbull) Winchcombe, Tarda, Flensburg, Tagish Lake, last visit 10 / 2022.
- [6] Daly L., King A.J., Joy K.H., Rowe J., UK Fireball Alliance, 2021. Elements, DOI: 10.2138/gselements.17.5.363.
- [7] Simms M.J., 2021. Geology Today, 37, 237-240.
- [8] <https://karmaka.de/?p=26757>: Winchcombe meteorite fall (2022).
- [9] Russell S.S., Salge T., King A., Daly L., Joy K., Bates H., Almeida N.V., Suttle M., Schofield P., UK Fireball Alliance Team, 2022. Microsc. Microanal. 28 (Suppl 1), 2732-2733.
- [10] Winchcombe meteorite fall 2021 in: 85<sup>th</sup> Annual Meeting of the Meteoritical Society 2022, contributions no: 6443, 6408, 6356, 6431, 6379, 6345, 6285, 6123, 6076, 6262, 6219.
- [11] Hoffmann V.H., et al. 2022a. Inter. Mineral. Congress, iposter # 1477.
- [12] Hoffmann V.H., et al. 2022b. Inter. Mineral. Congress, iposter # 1498.

## Asteroids as Localized Rocks with Mixed and Less Activity

Yasunori MIURA

*Department of Earth System Sciences, Faculty of Science, Yamaguchi University*

**Introduction:** Rocks beyond water-planet Earth have not discussed from those collection and laboratory classification comparatively because of less sampling projects through different celestial bodies widely in the Solar System. In order to make clear the differences with them including the Itokawa and the Rhygu Asteroids, the main points are described in this paper with short summary [1,2] (Table 1).

**Rocks as all different bodies and planets:** Planetary Earth System [3] is supported by fact that all different celestial bodies have different global data and collected meteorites, where activity factors of all rocks are different from aging data and variety of rock-type widely based on the youngest rocks of Earth (cf. Table 1).

**Localized and globally melted rocks:** All extreme condition are created by planet-type (volcano and quake) and by cosmic originated-types (impact and plasma), where the localized melted rocks are formed on all primordial bodies and planets including younger planet Earth. However, water-planet Earth shows the most active planet because of progressive global ocean-water system with dynamic separation of air-water-solid rock (VLS) phase widely to be possible for mixing and separation processes including purification to generate pure crystallized minerals and life with giant carbon-bearing molecules exclusively. In other words, planetary scientists should take care for any experiments on active space, reaction and description definitely (on volatile elements and molecule) including plasma-state reaction in any laboratory observation [1-8].

**Significant roles of global VLS system:** Although all localized impact event on all celestial bodies are produced a few melted and evaporated remains on the rock, the ranges are impacted areas with limited VLS growth during the melting. On the other hand, global VLS systems of Earth are produced solid system (continents and islands) changed as moved and changed with earthquake and volcano [5], and well-known geological impact layers [7,8] formed various kinds of rocks and many regional products. Therefore, local geological evidences produced regional products, however global system of Earth can form active factor of mixing and selection for rocks and life products exclusively [7,8]. Asteroids show limited mixing and selection of primordial products mainly.

**Complicated formation VLS products locally in Asteroids:** As there are evaporating elements and molecules beyond planet Earth, global VLS system of Earth are started as mixed grains of the VLS mixed micro-grains (as colloid solution and gel solid), which might be observed in the Asteroids separately as localized products (including plasma injection to the Asteroids' rocks). In Asteroids the localized products are the similar on the whole body with various impacts and injections [6,7,9,10].

**Carbon-bearing grains in Asteroids:** Carbon element is existed all meteorites and Asteroids micro- and macroscopically because it is stable molecules and solids after melting and pressing. Any Asteroids include texture of vacancy voids with carbon-bearing rims or grains formed by the plasma-injection (used by artificial technology). When it is formed mixed grains of colloids or quasi-solid, it might be remained in the rock's interior without separation (even at no global VLS system of any Asteroids), though mixed fluids are not pure water or CO<sub>2</sub> gas obtained in close system of Earth [2,5].

**Less active life formation beyond Earth in the Solar System:** Any mixed state grains with fluids are possible to bring to water planet or impacted planets under the room-temperature orbit zone even lower temperature as its unstable phase diagram. It might be exceptional case for mixed states of micro-gel states on the VLS planet Earth, where carbon-bearing VLS grains might kept in the void interiors of rock to produce pure water and CO<sub>2</sub> gas by slow and longer reaction process on dry Earth to water planet finally [11]. We can find carbon-bearing Egg shows mixed aggregates of colloidal solution and gel solids of organic compounds

in life-type event now (Table 1).

**Problem of observation and analyses:** The carbon and/or hydrogen-bearing grains under electron-beam or ion sputtering for longer experimental run which might be evaporated to reacted molecules (obtained at wide temperature). Impact-run collection to the Asteroids surface might be reacted between gun-metal with industry contamination (cf. metal with carbon buffer control to be broken at collected procedure) [7-9].

**Naming of minerals on Asteroids and any planets:** Mineral name is exclusively defined as well-crystallized end-products on globally VLS system of planet Earth. Therefore, mixed grains or reacted (at the Earth's experiments) are not used as its crystal name, but it is recommended to be used as fixed word before mineral names (cf. "celestial body name" + mineral) because of its mixture (especially volatile elements) [1,2].

**Summary:** The present results are summarized as follows:

- 1) Any rocks beyond Earth are not the same of water-planet Earth as mineral name used as paper, it should be used as adjective word before mineral names (cf. "celestial body name" + mineral) because of its mixture with volatile elements) for written paper.
- 2) All investigated rock data of planets and Asteroids previously are different in recorded database.
- 3) Melted rocks should take care for the effects from beam- and ion-sputtering naturally in the Solar System.
- 4) Local geology describes regional products, though global system of Earth can form active factor of mixing and selection processes for rocks and life products. Asteroids are the similar on the whole body by impacts and injections, where there is no global active factor triggered by the macro-ocean water system.
- 5) Carbon element is existed all meteorites and Asteroid, where they include texture of voids with carbon-bearing rims/grains formed by the plasma-injection as mixed grains of colloids, though mixed fluids are not pure water or CO<sub>2</sub> gas of Earth case.
- 6) Any mixed gel grain with fluids of Asteroids might be saved in the rocks globally. Carbon-bearing VLS grains might kept in the void interiors of rock to produce pure water and CO<sub>2</sub> gas by slow and longer reaction process on dry Earth to water planet.
- 7) The carbon and/or hydrogen-bearing grains under electron-beam or ion sputtering experimen might be evaporated to reacted molecules from previous impact-run collection.

Table.1 Characterization of mineral & life systems of Earth & extraterrestrial bodies.

Celestial bodies	Mineral	Life
Earth (water planet)	Earth Solid(3macro-VLS)	Water Earth (3micro-VLS)
Bodies (dry sites)	Returned &collected	No real samples (No fossil)

## References:

- [1] Miura Y. (2018) In Mineralogy past, present and future: preparing for the next 100 Years of the Mineral. Soc. America (IMA-22),1189. [2] Miura Y. (2022) Jour. Mineral. Petrol. Sci. (Japan) (submitted). [3] Wilson J.T. (1965) Nature, 207 (4995), 343-347. [4] Miura Y. (1996) In Shock-Wave Handbook (Springer-Verlag Tokyo),1073-1209. [5] Grove T.L. (2012) Ann. Review. Earth Planet. Sci. An. Rev. Earth and Planetary Sci. 40 (1), 413-439. [6] Miura Y. and Kato T. (1993) Amer. Inst. Physics (AIP) Conf. Proc., 283 (Earth & Space Sci. Inf. Systems), 488-492. [7] Miura Y. (1991) The Future of AMS (NSERC Grand. Carlisle Ed.), Vol.1, 45. [8] Miura Y. (1992) Celestial Mechanic. & Dynamical Astro. (Kluwer Academic), 54, 249-253. [9] Miura Y. (2008) Acta Crystal., 64, 55-55.[10] Miura Y. and Tomisaka T. (1984) Mem. Natl Inst. Polar Res., Spec. Issue (NIPR), 35, 210-225; 226-242. [11] Miura Y. (1994) The Astro. Soc. Pacific (ASP) Conf. Ser., 63, 259-264.

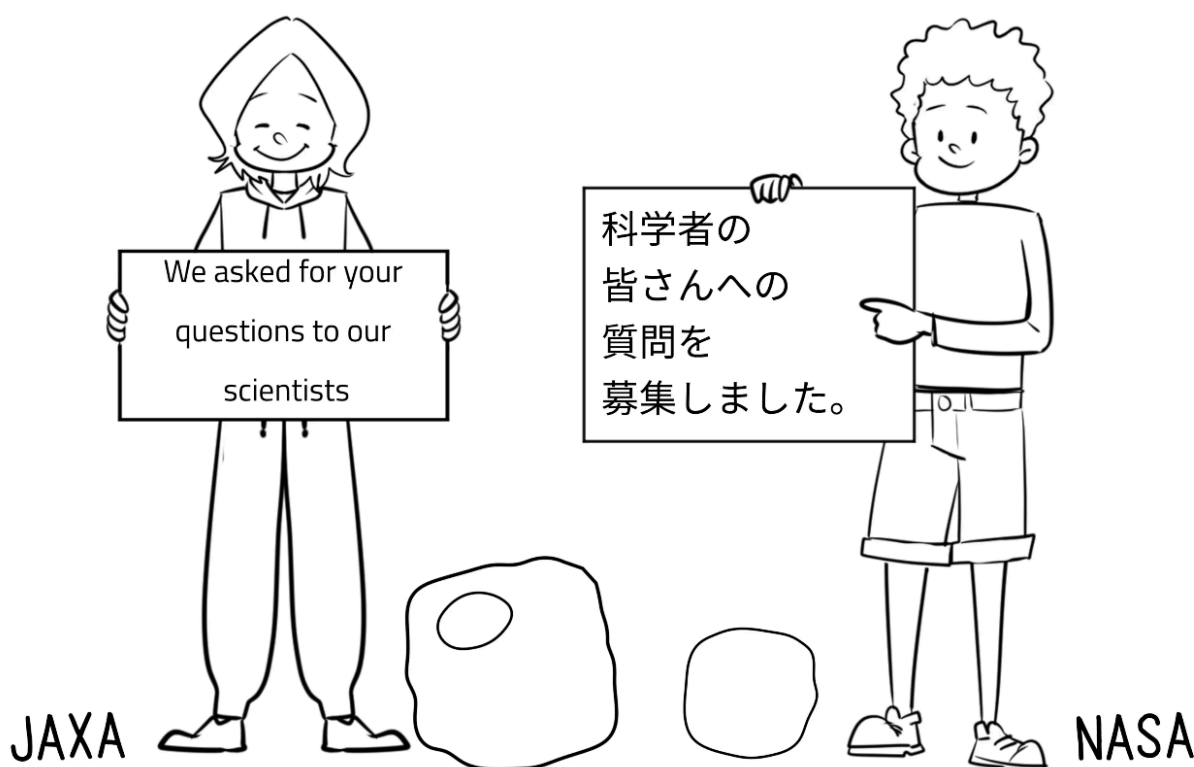
## Grains to Press: Outreach ideas for sharing analysis results from the Ryugu sample

Elizabeth Tasker, Makoto Yoshikawa, Ayumu Tokaji, Masaki Fujimoto  
*ISAS/JAXA*

Planetary science missions are sometimes described as “science theatre” due to often having a series of big events such as launch, arrival and touchdown that can be leveraged to share scientific and engineering mission news with a broad audience. While publishing accurate and timely information remains challenging during a mission, images from the spacecraft can often be quickly appreciated, and act as a gateway to sharing more in-depth content. It is more difficult to keep up this dissemination of information during the sample analysis stage, where the careful work required (and the publication process itself) means that timing of the results cannot be controlled, the images not so quickly understood, and the conclusions one part of a large jigsaw puzzle being performed that may initially offer contradictions.

The information we discover from the analysis of the sample from asteroid Ryugu is the reason that Hayabusa2 flew. The questions being tackled concerning the origins of life are relevant to everyone on Earth, and the mission has generated strong interest in what might be discovered in the grains. Therefore, it is important that we meet this additional mission challenge to develop outreach material that can explain the process of the analysis, and share results in a way that is interesting and accurate.

This talk takes a look at some of the material used at ISAS to share information about the analysis, including videos, articles and Q&A events on social media. Suggestions will be asked for (be ready!) and ideas about the content that could be shared as we unpick the secrets held in this sample, and prepare for the sample from asteroid Bennu.



(Snapshot from the video on the Ryugu/Bennu social media Q&A)

# TOF-SIMS analysis of macromolecular organic matter in Ryugu samples

M. Hashiguchi<sup>1</sup>, D. Aoki<sup>1</sup>, K. Fukushima<sup>1</sup>, H. Yabuta<sup>2</sup>, H. Yurimoto<sup>3</sup>, T. Nakamura<sup>4</sup>, T. Noguchi<sup>5</sup>, R. Okazaki<sup>6</sup>, H. Naraoka<sup>6</sup>, K. Sakamoto<sup>7</sup>, S. Tachibana<sup>7,8</sup>, S. Watanabe<sup>1</sup>, Y. Tsuda<sup>7</sup> and the Hayabusa2-initial-analysis IOM team

<sup>1</sup>Nagoya University, Nagoya, 464-8601, Japan, <sup>2</sup>Hiroshima University, Higashi-Hiroshima, 739-8526, Japan, <sup>3</sup>Hokkaido University, Sapporo, 001-0021, Japan, <sup>4</sup>Tohoku University, Sendai, 980-8577 Japan, <sup>5</sup>Kyoto University, Kyoto, 606-8501, <sup>6</sup>Kyushu University, 819-0395, Japan, <sup>7</sup>ISAS/JAXA, Sagami-hara, 252-5210, Japan, <sup>8</sup>The University of Tokyo, Bunkyo-ku, 113-8654, Japan.

**Introduction:** The Hayabusa2 spacecraft returned samples with total mass of ~5 g from surface of asteroid Ryugu in December 2020 [1]. Chamber A aggregates collected upon the first touchdown and chamber C aggregates collected upon the second touchdown were investigated by the Hayabusa2 initial analysis team from June 2021 to May 2022.

The initial analysis organic macromolecule team has performed chemical, molecular, and isotopic analysis on the intact Ryugu grains and insoluble organic matter (IOM) isolated from Ryugu samples by  $\mu$ -FTIR, micro-Raman spectroscopy, STXM-XANES, STEM-EELS, AFM-IR, and NanoSIMS [e.g., 4–8]. The result showed that chemical and isotopic compositions are broadly similar between Ryugu IOM and CI chondritic IOM, although some differences between the two IOM were reported by FTIR.

Time-of-Flight Secondary Ion Mass Spectrometry (TOF-SIMS) is useful to analyze the molecular species present on the sample surface. This technique has been applied for a variety of organic matter from macromolecular materials [e.g., 9] and extraterrestrial samples [e.g., 10–11]. In this study, we conducted in-situ analysis on bulk Ryugu samples and the isolated IOM using TOF-SIMS to investigate the chemical structure of macromolecular organic matter in asteroid Ryugu.

**Experimental:** IOM were extracted from two Ryugu aggregate samples (A0106 and C0107) with 6M HCl and 1M HCl/9M HF at Hiroshima University [4]. Those Ryugu IOM samples and intact Ryugu grains A0106 and C0057 were used in this study. For comparison, Tagish Lake IOM and bulk samples of Tagish Lake (C-ungrouped) and Orgueil (CI) were used. All those samples were pressed onto clean copper disks (~2.1 mm $\phi$ ) and mounted in in-house stainless steel holder for TOF-SIMS analysis. Roughness of the sample surface and copper disks were < 10  $\mu$ m for fragment samples, < 5  $\mu$ m for IOM samples, respectively. The TOF-SIMS measurement was performed using a TRIFT III spectrometer (ULVAC-PHI, Inc., Chigasaki, Kanagawa, Japan) at Nagoya University. Positive and negative ion spectra were obtained using Au<sup>+</sup> gold primary ion (22 keV, 1.2 nA). The measured surface areas were 200  $\times$  200  $\mu$ m and acquisition time of about 5 min for each sample. The ion intensity of each species was obtained from region of interest (ROI) of the sample of all samples, and were normalized by using total ion intensity of signals at  $m/z$  0 to 150. After the TOF-SIMS analysis, mineralogical observation was performed on the sample using SEM/EDS.

**Results and Discussions:** Various ions derived from hydrocarbon moieties (C<sub>n</sub>H<sub>x</sub><sup>+</sup>), which containing 1-10 carbons, were detected from both of extracted IOM and bulk samples from asteroid Ryugu samples and Tagish Lake and Orgueil meteorites at  $m/z$  10–150 of TOF-SIMS spectra.

Normalized intensities of these fragment ions and the fragment patterns were almost similar between A0106 and C0107 IOM. Most abundant fragment ion was C<sub>2</sub>H<sub>3</sub><sup>+</sup> or C<sub>2</sub>H<sub>5</sub><sup>+</sup> for both extracted IOM and bulk samples from Ryugu and Tagish Lake. Lower mass fragment ions (C<sub>1</sub>~C<sub>4</sub>) were more abundant than higher mass fragment ions for both Ryugu and the carbonaceous chondrite samples. Furthermore, intensity of C<sub>n</sub>H<sub>2n+1</sub><sup>+</sup> ( $n=1\sim4$ ) and C<sub>n</sub>H<sub>2n-1</sub><sup>+</sup> ( $n=3\sim5$ ) ions from Ryugu IOM were higher than from Tagish Lake IOM. This trend implies that Ryugu IOM contains more abundant hydrogen than Tagish Lake IOM. On the other hand, Tagish Lake IOM showed higher intensity of C<sub>n</sub>H<sub>2n+1</sub><sup>+</sup> ( $n>5$ ) and/or C<sub>n</sub>H<sub>2n-1</sub><sup>+</sup> ( $n>6$ ) ions than Ryugu IOM. Although it is not clear whether these ions are derived from aromatic carbon or aliphatic carbon, the high mass fragment ions would indicate the presence of aromatic rings [12]. A previous TOF-SIMS study suggests that C<sub>n</sub>H<sub>2</sub><sup>+</sup> radical cations and C<sub>n</sub><sup>-</sup> radical anions are the fragmentation ions derived from aromatic moieties [12]. In this study, these radical cations or anions were detected from both Ryugu and Tagish Lake IOM, while their abundances from Tagish Lake IOM were higher than those from Ryugu IOM, except C<sub>5</sub>H<sub>2</sub><sup>+</sup>. The result suggests that Ryugu IOM is less molecularly evolved relative to Tagish Lake IOM, which is consistent with the solid-state <sup>1</sup>H-NMR results for organic matter in Ryugu samples [13]. Also, the abundances of intensity of C<sub>n</sub><sup>-</sup> radical anions from the bulk Ryugu samples were lower than those from Tagish Lake, which also supports our observation for the extracted IOM.

Compared to bulk samples of Tagish Lake and Orgueil, it was hard to see clear difference on hydrocarbon fragment ions such as their intensity and H/C ratio between Ryugu samples like result of IOM samples, except  $C_5H_x^+$ . This may probably be due to sample heterogeneity. However, Tagish Lake and Orgueil bulk samples showed clearly developed  $C_5H_x^+$  peaks relative to the bulk Ryugu samples. On the other hand, the extracted IOM showed the opposite trend: the peak intensities of  $C_5H_x^+$  ions from Ryugu IOM, especially  $C_5H_7^+$ , were very high relative to those from Tagish Lake IOM. Such a large difference between bulk sample and IOM from the same sample has not been observed from meteorites, and therefore the observation implies the different chemical structures of Ryugu IOM and organic matter from bulk samples, which could be result from the acid-susceptible nature of the Ryugu samples. Different chemical structure of organic matter between Ryugu and Tagish Lake may result from freshness of Ryugu organic matter with no or little terrestrial alteration and/or different aqueous alteration process. Further TOF-SIMS analysis on CI chondrite IOM will provide more detailed firm interpretation for chemical evolution of Ryugu OM.

### Acknowledgements

We thank to Mr. R. Nishimura at Nagoya University for making in-house holder for TOF-SIMS analysis in this study.

### References

- [1] Yada T. *et al.* (2021) *Nat. Astron.* 6, 214–220. [2] Arakawa M. *et al.* (2020) *Science*, 368, 67–71. [3] Tsuda, Y. *et al.* (2020), *Acta Astronautica* 171, 42–54, 2020. [4] Yabuta H. *et al.* (2022) *Science, in revision*. [5] Kebukawa Y. *et al.* (2022) 53<sup>rd</sup> LPSC. #1271. [6] Stroud R. M. *et al.* (2022) 53<sup>rd</sup> LPSC. #2052. [7] Remusat L. *et al.* (2022) in 53<sup>rd</sup> LPSC. #1448. [8] Quirico E. *et al.* (2022) *this meeting*. [9] Stephan T. *et al.* (2003), *Meteorit. & Planet.Sci.* 38, 109–116. [10] Noun M. *et al.* (2020) *Life*, 9, p.44. [11] Hashiguchi M. *et al.* (2022) 53<sup>rd</sup> LPSC. #1867. [12] Sjövall P *et al.* (2021) *Fuel*, 286, 119373. [13] Cody G. D. *et al.* (2022) *this meeting*.

## Continuing preparations for NASA curation of the OSIRIS-REx asteroid sample

N.G. Lunning<sup>1</sup>, K. Righter<sup>1</sup>, R. C. Funk<sup>2</sup>, C.S. Snead<sup>1</sup>, W. D. Connelly<sup>2</sup>, S. Martinez<sup>2</sup>, M. Montoya<sup>2</sup>, J. L. Plummer<sup>2</sup>,  
K. K. Alums<sup>2</sup>, M. Rodriguez<sup>2</sup>,

<sup>1</sup>*Astromaterials Curation, NASA Johnson Space Center, 2101 NASA Pkwy, Houston, TX 77058 USA*

<sup>2</sup>*Jacobs/JETS, Astromaterials Curation, NASA Johnson Space Center, 2101 NASA Pkwy, Houston, TX 77058 USA*

The OSIRIS-REx spacecraft collected an estimated 250-gram asteroid sample, completed its Bennu asteroid operations phase, and is on its way to return the asteroid sample to Earth on September 24, 2023 [1]. Construction of the OSIRIS-REx curation cleanroom (ISO 5) at NASA Johnson Space Center was completed in late 2021 and has been subject to ongoing monitoring for contamination knowledge [2,3]. The OSIRIS-REx curation cleanroom is inside of a lab suite with pass-throughs to an adjacent staging area and to an adjacent microtomy lab (ISO 7), which also separate it from the NASA Hayabusa2 cleanroom (ISO 5). In addition, a non-cleanroom space (OSIRIS-REx section lab) was built outside of the cleanroom suite for anticipated sample preparation activities that cannot be conducted in the curation cleanroom. Preparations for sample recovery and curation build on work that spans most of the last decade [e.g., 4] This presentation will cover curation preparation for the OSIRIS-REx sample over the last few years and plans for curation immediately following Earth return.

### Recovery

The OSIRIS-REx curation team is involved in detailed planning for recovery of the sample return capsule (SRC) at the Utah Testing and Training Range (UTTR). This planning and preparation builds on lessons learned from the Genesis and Stardust recovery operations that also took place at UTTR. Our preparations involve plans for both nominal and off-nominal landing scenarios. For off-nominal landing scenarios, as a lesson learned from the environmental sensitivity of the returned Ryugu samples, a substantial factor is the potential sensitivity of the returned Bennu asteroid sample to environmental contamination and degradation, which may be much greater than that of the Genesis and Stardust samples. This includes the importance of, as rapidly as safe and feasible, getting the returned sample onto a nitrogen gas (GN2) purge to protect it from oxygen and humidity. In nominal landing scenarios, the sample canister that includes the Touch-And-Go Sample Acquisition Mechanism (TAGSAM) head will be flown from Utah to Houston for further disassembly at NASA JSC.

### Spacecraft disassembly at NASA JSC

In Houston, the sample canister will remain under GN2 purge until it is transferred to a GN2 glovebox in the OSIRIS-REx curation cleanroom. The sample canister will be opened inside of a glovebox that was specifically designed to accommodate removing its lid. The curation team has been rehearsing this process and other hardware disassembly and sample handling processes in glovebox mockups to refine disassembly techniques. In addition, rehearsals are helping to prepare the team for the intense hardware and sample handling that will occur during preliminary examination (PE). After the sample canister lid is removed, the TAGSAM head will be revealed and its condition documented. It is unknown to what extent Bennu dust will have migrated from inside the TAGSAM head outward to cover the interior of the canister lid. Shortly after documentation of the interior of the canister lid and the exterior of the TAGSAM head, the TAGSAM head will be removed and weighed on a stand. The nominal weight of the empty TAGSAM (and the stand) will be subtracted from the weight of the returned TAGSAM head holding sample to get the first estimate of the mass of the returned bulk sample. Next, the TAGSAM head will be sealed inside of a transfer container and moved to a second specially designed glovebox for further documentation and disassembly.

The first operations in the glovebox designed for TAGSAM head disassembly will focus on the contact pads, which have been previously described [5]. The contact pads and associated particles will be visually examined, carefully documented in place, relevant hardware will be further disassembled, then the contact pads will be removed and containerized. Following containerization of the contact pads, disassembly of the TAGSAM head will continue until only several components remain holding the returned asteroid sample. At this point the sample will be gently poured off the remaining hardware, which will be followed by documentation of the bulk sample poured from inside the TAGSAM head into a set of trays for more detailed imagery and storage. The containers that returned samples, contact pads, and flight witness plates are stored inside of will be tested to quantify the time interval they are able to maintain an anoxic environment outside of a curation glovebox [6].

Laboratory monitoring described by [3] will continue throughout PE (the six months of after Earth return) and beyond. In addition, witness plates will be deployed to monitor the interiors of gloveboxes in which the spacecraft hardware will be disassembled and asteroid samples will be processed.

## Catalog Release

PE will culminate in the initial public release of the OSIRIS-REx returned sample catalog around the end of March 2024. We anticipate the OSIRIS-REx return sample catalog will grow over time as more individual particles undergo basic characterization. After the release of the catalog in March 2024, the collection will be open for sample requests from the entire community. As is the case for all NASA's astromaterials collections, a collection-specific allocation board will be convened to review OSIRIS-REx sample requests.

## **References**

[1] Lauretta, D. S., Adam, C. D., Allen, A. J., Ballouz, R. L., Barnouin, O. S., Becker, K. J., Becker, T., Bennett, C. A., Bierhaus, E. B., Bos, B. J. and Burns, R. D., 2022. Spacecraft sample collection and subsurface excavation of asteroid (101955) Bennu. *Science*, 377(6603), pp.285-291 [2] Dworkin J. P., Adelman L. A., Ajluni T., Andronikov A. V., Aponte J. C., Bartels A. E., Beshore E., Bierhaus E. B., Brucato J. R., Bryan B. H., Burton A. S., Callahan M. P., Castro-Wallace S. L., Clark B. C., Clemett S. J., Connolly H. C., Cutlip W. E., Daly S. M., Elliott V. E., Elsilá J. E., Enos H. L., Everett D. F., Franchi I. A., Glavin D. P., Graham H. V., Hendershot J. E., Harris J. W., Hill S. L., Hildebrand A. R., Jayne G. O., Jenkins R. W., Johnson K. S., Kirsch J. S., Lauretta D. S., Lewis A. S., Loiacocono J. J., Lorentson C. C., Marshall J. R., Martin M. G., Matthias L. L., McLain H. L., Messenger S. R., Mink R. G., Moore J. L., Nakamura-Messenger K., Nuth J. A., Owens C. V., Parish C. L., Perkins B. D., Pryzby M. S., Reigle C. A., Righter K., Rizk B., Russell J. F., Sandford S. A., Schepis J. P., Songer J., Sovinski M. F., Stahl S. E., Thomas-Keprta K., Vellinga J. M., and Walker M. S..2018. OSIRIS-REx Contamination Control Strategy and Implementation. *Space Science Review* 214, 1-19. [3] Righter, K., Lunning, N.G., Snead, C.S., 2022. Contamination monitoring of the OSIRIS-REx ISO5 asteroid sample cleanroom. this symposium. [4] Righter, K. and Nakamura-Messenger, K., 2017. Sample curation in support of the OSIRIS-REx asteroid sample return mission. Hayabusa Symposium. [5] Bierhaus E. B., Clark B. C. Harris J. W., Payne K. D., Dubisher R. D., Wurts D. W., Hund R. A., Kuhns, Linn T. M., Wood J. L., May A. J., Dworkin J. P., Beshore E., Lauretta D. S., and the OSIRIS-REx Team. 2018. The OSIRIS-REx spacecraft and the Touch-and-Go sample acquisition mechanism (TAGSAM). *Space Science Reviews* 214, 1-46. [6] Snead, S. C., Righter, K., Lunning, N. G., 2022., this symposium.